Applied Mathematical Modelling 96 (2021) 657–677

Contents lists available at ScienceDirect

Applied Mathematical Modelling

journal homepage: www.elsevier.com/locate/apm

Elastic buckling and free vibration analysis of functionally graded Timoshenko beam with nonlocal strain gradient integral model

Yuan Tang, Hai Qing*

State Key Laboratory of Mechanics and Control of Mechanical Structures, Nanjing University of Aeronautics and Astronautics, Nanjing 210016, China

ARTICLE INFO

Article history:
Received 17 December 2020
Revised 29 January 2021
Accepted 17 March 2021
Available online 27 March 2021

Keywords:
Elastic buckling
Free vibration
Size-dependent
Nonlocal strain gradient integral model
Integro-differential equations
Laplace transform technique

ABSTRACT

In this work, nonlocal strain gradient integral model is applied to study the elastic buckling and free vibration response of functionally graded (FG) Timoshenko beam which is made of two constituents varying along thickness direction. The differential governing equations and corresponding boundary conditions are derived via the Hamilton's principle, and the relations between nonlocal stresses and strains are expressed as integral equations. The Laplace transform technique is applied to solve directly the integro-differential equations, and the explicit expression for bending deflections and moments, as well as cross-sectional rotation and shear force is expressed with eight unknown constants. The nonlinear characteristic equations to determine the characteristic buckling load and vibration frequency are derived explicitly in consideration of corresponding boundary conditions and constitutive constraints. The buckling load and vibration frequency from present model are validated against to the existed results in literature. Consistent softening and toughening responses with respect to length-scale parameters can be obtained.

1. Introduction

Beam-like structures are widely applied in microelectromechanical and nanoelectromechanical systems, such as actuators [1], sensors [2], resonators [3], transistors [4], probes [5] and so on. Therefore there is a growing desire in analyzing the dynamic behavior of micro- and nano-beam components. Previous studied show that both softening and toughening effects can be observed for micro- and nano-scale structures [6–9], and mechanical analysis should address size-dependent behaviors.

In 1960s, Koiter [10], Toupin [11] as well as Mindlin and Tiersten [12] proposed classic couple stress models, and Mindlin [13,14] proposed the strain gradient elasticity. The higher-order deformation mechanisms are taken into account in both couple stress model and strain gradient model. Later, Lam et al. [15] and Yang et al. [16] presented a modified strain gradient model and couple stress model, respectively. With the application of strain gradient and couple stress models, the toughening effect of materials-length scale parameter on the mechanical response of micro- and nano-scale structures and materials can be observed, such as the buckling loads and vibration frequencies of micro- and nano-scale beams [17–22].

* Corresponding author.
E-mail address: qinghai@nuaa.edu.cn (H. Qing).

https://doi.org/10.1016/j.apm.2021.03.040
0307-904X/

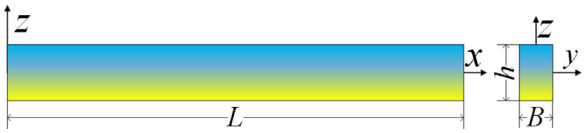

Fig. 1. Geometrical scheme of FG beam.

Over almost same period, the nonlocal elasticity was proposed initially by Kroner [23] and improved by Eringen and his colleagues [24,25]. The softening effect of materials-length scale parameter on the structural mechanical response can be observed while using nonlocal model, for example [26–31].

Combining nonlocal integral model and strain gradient model, Lim et al. [32] proposed a nonlocal strain gradient model which is expected to address both softening and toughening effects. Nonlocal strain gradient model is widely applied to investigate the size-dependent response of micro- and nano-scale structures. Ebrahimi and Barati applied a higher order refined beam model to investigate the damping vibration response of FG-beam embedded in Winkler–Pasternak foundation [33] and buckling behavior of a curved FG-beam [34]. With the application of two-stepped perturbation technique, Sahmani and Aghdam [35] and Sahmani et al. [36] studied the nonlinear vibration and bending of axially-loaded multilayer FG composite nanobeams, She et al. [37] studied the nonlinear bending and vibrational behaviors of FG microtubes, and Gao et al. [38] studied the nonlinear vibration of FG nanotube. Al-shujairi and Mollamahmutoglu [39] applied general differential quadrature method (GDQM) to study the influence of the thermal effects on dynamic stability of FG Timoshenko sandwich microbeam. Liu et al. [40] studied the nonlinear free vibration of sandwich Euler–Bernoulli beams with initial deflection. Guo et al. [41] applied Galerkin approach to study transverse vibration and vibro-buckling characteristics of axially moving and rotating simply supported Euler–Bernoulli beam. Lu et al. [42] derived the analytical solutions for buckling load of rectangular plate on different higher-order plate theories, and studied the influence of geometric parameters, boundary conditions and shear deformation on the buckling loads of rectangular plate. Li and Hu [43] and Li et al. [44] studied the influence of through-thickness power-law variation and size-dependent parameters on the free vibration of simply supported Euler–Bernoulli and Timoshenko beam. Mohammadian et al. [45] applied nonlocal strain gradient Timoshenko beam model to study the dynamic behavior of the hetero junction carbon nanotubes. Karami et al. [46] applied GDQM to study the free vibration of bi-directionally FG Timoshenko beam with tapered cross-section. Mir and Tahani [47] applied Kirchhoff plate to model graphene sheet resonator, and employed Melnikov integral method to deduce the analytical criteria for oscillation chaos.

However, the studies of Zaera et al. [48] and Li et al. [49] show the inconsistency occurs for static bending of Euler–Bernoulli beam. In this paper, the nonlocal strain gradient integral model is applied to model the elastic buckling and free vibration of FG Timoshenko beam which is made of two constituents varying along thickness direction, and the consistency of dynamic response of FG Timoshenko beam is checked for the first time. The differential governing equations and boundary conditions are derived via the Hamilton's principle. The differential governing equation and integral constitutive equation are solved directly with the Laplace transform technique, and the explicit expression for bending deflections and moments as well as cross-sectional rotation and shear force is derived uniquely with eight unknown constants. In consideration of the boundary conditions and constitutive constraints, the nonlinear characteristic equations about buckling load and vibration frequency are derived explicitly. The influence of FG exponent index, length-scale parameters, boundary conditions, ratio between length and thickness as well as buckling and vibration orders on the buckling load and vibration frequency is investigated numerically.

2. Mathematical formulation

2.1. Functionally graded material

Fig. 1 illustrates a FG Timoshenko beam of length L, width B and thickness h. The FG beam is assumed to be made of aluminum and the ceramic at bottom and top surfaces, whose volume fraction follows the power law along thickness direction as

$$v_c(z) = (z/h + 1/2)^k,\ v_a(z) = 1 - v_c(z) \tag{1}$$

in which, the variables with subscripts a and c indicate data for aluminum and the ceramic, respectively.

According to the Mori–Tanaka homogenization scheme [50], the effective bulk modulus K_e and shear modulus G_e are given by

$$\begin{aligned} \frac{K_e - K_a}{K_c - K_a} &= \frac{v_c(z)}{1 + v_a(z)(K_c - K_a)/(K_a + 4G_a/3)} \\ \frac{G_e - G_a}{G_c - G_a} &= \frac{v_c(z)}{1 + v_a(z)(G_c - G_a)/[G_a(1 + (9K_a + 8G_a)/(6K_a + 12G_a))]} \end{aligned} \tag{2}$$

in which, the bulk modulus K and shear modulus Gcan be expressed in Young's modulus E and Poisson's ratio υ as

$$\begin{aligned} G &= E/[2(1+\upsilon)] \\ K &= E/[3(1-2\upsilon)] \end{aligned} \tag{3}$$

Combining of Eqs. (3) and (2), one can express the effective Young's modulus as

$$E_e = 9K_eG_e/(3K_e + G_e) \tag{4}$$

Therefore, the position of neutral plane can be determined as [33]

$$h_0 = \int_A zE_e dA / \int_A E_e dA \tag{5}$$

in which, A is beam cross-sectional area. According to the rule of mixture, the effective density ρ_e is given by

$$\rho_e = \rho_a v_a(z) + \rho_c v_c(z) \tag{6}$$

One can further calculate the mean Young's and shear moduli as well as density for homogeneous material with same volume fraction

$$\begin{aligned} \underline{E} &= \int_A E_e dA/A \\ \underline{G} &= \int_A G_e dA/A \\ \underline{\rho} &= \int_A \rho_e dA/A \end{aligned} \tag{7}$$

2.2. Governing equation of Timoshenko beam

The displacement field for an FG-Timoshenko beam is assumed to be

$$\begin{cases} u_x = (z-h_0)\phi(x,t) \\ u_y = 0 \\ u_z = w(x,t) \end{cases} \tag{8}$$

where, w and ϕ are the bending deflection and cross-sectional rotation, respectively. The corresponding nonzero strain components are

$$\varepsilon_x = (z-h_0)\phi', \varepsilon_{zx} = (\phi + w')/2 \tag{9}$$

The variation of the strain energy in the period from 0 to T is

$$\delta U = \int_0^T \int_v (\sigma_x \delta\varepsilon_x + 2\sigma_{xz}\delta\varepsilon_{xz}) \mathrm{d}v\mathrm{d}t = \int_0^T \left[M\delta\phi|_0^L + V\,\delta w|_0^L + \int_0^L (V - M')\delta\phi - V'\delta w \mathrm{d}x \right] \mathrm{d}t \tag{10}$$

where, σ_x and σ_{xz} are the nonlocal stress components and

$$\begin{cases} M = \int_A (z-h_0)\sigma_x \mathrm{d}A \\ V = \int_A \sigma_{xz} \mathrm{d}A \end{cases} \tag{11}$$

The variation of work in the period from 0 to T due to axial compressive force P can be expressed as

$$\delta W = \int_0^T \int_0^L Pw'\delta w' dx\mathrm{d}t = \int_0^T (Pw'\,\delta w|_0^L - \int_0^L Pw''\delta w dx)\mathrm{d}t \tag{12}$$

The variation of kinetic energy due to transverse vibration in the period from 0 to T can be given as

$$\delta K = \int_0^T \int_0^L \rho A\dot{w}\delta\dot{w}\mathrm{d}x\mathrm{d}t = \int_0^L \rho A\dot{w}\,\delta w|_0^T \mathrm{d}x - \int_0^T \int_0^L \rho A\ddot{w}\delta w \mathrm{d}x\mathrm{d}t \tag{13}$$

Based on the Hamilton's principle, the differential governing equations and boundary conditions can be respectively expressed as

$$\begin{cases} V - M' = 0 \\ V' - Pw'' - m\ddot{w} = 0 \end{cases} \tag{14}$$

$$\begin{cases} (V - Pw')\,\delta w|_0^L = 0 \\ M\,\delta\phi|_0^L = 0 \end{cases} \tag{15}$$

in which,

$$m = \int_A \rho_e \mathrm{d}A = \underline{\rho}A \tag{16}$$

2.3. Nonlocal strain gradient integral model

On the basis of nonlocal strain gradient integral model, the relations between nonlocal stresses and strains in a Timoshenko beam are

$$\sigma_{zx}(x,t)=\frac{\xi}{2\kappa}\int_0^L \tau_{zx}(\eta,t)\mathrm{e}^{-\frac{|x-\eta|}{\kappa}}d\eta-\frac{c^2}{2\kappa}\frac{\partial}{\partial x}\int_0^L \tau'_{zx}(\eta,t)\mathrm{e}^{-\frac{|x-\eta|}{\kappa}}d\eta \tag{17}$$

in which, κ and c are length-scale parameters related to nonlocal and strain gradient effects, respectively, while τ_x and τ_{zx} are local stresses which are given as

$$\tau_x=E_e\varepsilon_x,\ \tau_{zx}=2G_ek_s\varepsilon_{zx} \tag{18}$$

in which, k_s is the shear correction factor.

Combination of Eqs. (17)–(18) with (9) gives

$$\begin{aligned}\frac{M(x,t)}{EI}&=\frac{1}{2\kappa}\int_0^L \phi'(\eta,t)\mathrm{e}^{-\frac{|x-\eta|}{\kappa}}d\eta-\frac{c^2}{2\kappa}\frac{\partial}{\partial x}\int_0^L \phi''(\eta,t)\mathrm{e}^{-\frac{|x-\eta|}{\kappa}}d\eta\\ \frac{V(x,t)}{GA}&=\frac{1}{2\kappa}\int_0^L \left[w'(\eta,t)+\phi(\eta,t)\right]\mathrm{e}^{-\frac{|x-\eta|}{\kappa}}d\eta-\frac{c^2}{2\kappa}\frac{\partial}{\partial x}\int_0^L \left[w''(\eta,t)+\phi'(\eta,t)\right]\mathrm{e}^{-\frac{|x-\eta|}{\kappa}}d\eta\end{aligned} \tag{19}$$

in which,

$$EI=\int_A E_e(z-h_0)^2\mathrm{d}A,\ GA=k_s\int_A G_e\mathrm{d}A=k_s\underline{G}A \tag{20}$$

Clearly, Eq. (19) is the 1st kind Fredholm type integral equations.

Performing Laplace transformation respect to x on Eq. (19) and taking into account the results of Bian and Qing [51], one gets

$$\begin{aligned}\kappa^2\frac{\mathcal{L}\{M\}}{EI}&=\left(c^2-\frac{\kappa^2-c^2}{\kappa^2s^2-1}\right)\mathcal{L}\{\phi'\}+\frac{C_1}{\kappa s-1}+\frac{C_2}{\kappa s+1}\\ \kappa^2\frac{\mathcal{L}\{V\}}{k_sGA}&=\left(c^2-\frac{\kappa^2-c^2}{\kappa^2s^2-1}\right)\left(\mathcal{L}\{w'\}+\mathcal{L}\{\phi\}\right)+\frac{C_3}{\kappa s-1}+\frac{C_4}{\kappa s+1}\end{aligned} \tag{21}$$

in which, $\mathcal{L}$ is Laplace operator, and

$$\begin{cases}C_2=-\dfrac{\kappa c^2}{2}\phi'(0,t)\\ C_4=-\dfrac{\kappa c^2}{2}(\phi(0,t)+w'(0,t))\end{cases} \tag{22}$$

$$\begin{cases}C_1=\dfrac{\kappa^2-c^2}{2}\displaystyle\int_0^L \phi'(x,t)\mathrm{e}^{-x/\kappa}\mathrm{d}x-\frac{\kappa c^2}{2}\phi'(L,t)\mathrm{e}^{-L/\kappa}\\ C_3=\dfrac{\kappa^2-c^2}{2}\displaystyle\int_0^L (\phi(x,t)+w'(x,t))\mathrm{e}^{-x/\kappa}\mathrm{d}x-\frac{\kappa c^2}{2}(\phi(L,t)+w'(L,t))\mathrm{e}^{-L/\kappa}\end{cases} \tag{23}$$

3. Elastic buckling of nonlocal strain gradient Timoshenko beam

In this section, the theoretical solutions for elastic buckling of nonlocal gradient Timoshenko beam are derived subjected to the boundary conditions. The boundary conditions at one end, let us say x =0, can be classified as the four types from Eq. (15):

- Clamped end: $w(0,t)=\phi(0,t)=0$
- Hinged end: $w(0,t)=M(0,t)=0$
- Guided end: $V(0)-Pw'(L)=\phi(0)=0$
- Free end: $V(0)-Pw'(L)=M(0)=0$

In this study, six types of boundary condition combination shown in Table 1 are taken into account. Neglecting the inertial effect and time variable, the governing equations (14) for elastic buckling of Timoshenko beam can be expressed as

$$\begin{cases}V-M'=0\\ V'-Pw''=0\end{cases} \tag{24}$$

Table 1
Boundary conditions for Timoshenko beam.

Boundary conditions	Equations
Simply-Supported (SS)	$w(0) = M(0) = w(L) = M(L) = 0$
Hinged-Clamped (SC)	$w(0) = M(0) = w(L) = \phi(L) = 0$
Hinged-Guided (SG)	$w(0) = M(0) = V(L) - Pw'(L) = \phi(L) = 0$
Clamped–Clamped (CC)	$w(0) = \phi(0) = w(L) = \phi(L) = 0$
Clamped-Free (CF)	$w(0) = \phi(0) = M(L) = V(L) - Pw'(L) = 0$
Clamped-Guided (CG)	$w(0) = \phi(0) = \phi(L) = V(L) - Pw'(L) = 0$

Performing Laplace transformation respect to x on Eq. (24) and taking into account Eq. (21), one gets

$$\begin{aligned}\mathcal{L}\{w\} = \{&s^5C_7\kappa^2(pL^2\kappa^2 - c^2EI\Omega) - s^4\kappa\left[C_5L^2\kappa^3 - EI(C_3 + C_4 + c^2\kappa C_8)\right]\\ &-s^3\left[EI\Omega(C_4 - C_3 + C_1\kappa + C_2\kappa - C_7\kappa^2) + C_7\kappa^2L^2p - C_6\kappa^4\Omega\right]\\ &-s^2\left[EI\Omega(C_1 - C_2 + C_8\kappa^2) - C_5\kappa^2(L^2 + \kappa^2\Omega)\right] - \kappa^2\Omega(C_6s + C_5)\}/\\ &\left[s^2(s^2 - \alpha_v^2)(s^2 - \beta_v^2)\kappa^2(pL^2\kappa^2 - c^2EI\Omega)\right]\end{aligned} \tag{25}$$

$$\begin{aligned}\mathcal{L}\{\phi\} = \{&s^6C_8EI\kappa^2c^2(c^2EI\Omega - pL^2\kappa^2) + s^5\kappa(c^2EI\Omega - pL^2\kappa^2)[(C_6 + pC_7)\kappa^3\\ &- EI(C_1 + C_2)] + s^4EI[(C_1 - C_2 + C_8\kappa^2)(pL^2\kappa^2 - c^2EI\Omega) + \kappa^2c^2C_8(pL^2 - EI\Omega)\\ &- \kappa^3\Omega(C_3p + C_4p - C_8\kappa c^2)] + s^3\kappa[(C_1 + C_2)EI(EI\Omega - pL^2) + (C_6 + pC_7)(2pL^2\kappa^3\\ &- \kappa EI(\kappa^2 + c^2)\Omega) + p\kappa(C_4 - C_3)EI\Omega] - s^2EI[(C_1 - C_2 + C_8\kappa^2)(pL^2 - EI\Omega)\\ &+ C_5\kappa^2(\kappa^2 + c^2) - p\kappa(C_3 + C_4)] + s[(C_3 - C_4)EIp\Omega - (C_6 + pC_7)\kappa^2(pL^2 - EI\Omega)]\\ &+ \kappa^2EI\Omega C_5\}/\left[s(c^2s^2 - 1)(s^2 - \alpha_v^2)(s^2 - \beta_v^2)\kappa^2EI(c^2EI\Omega - pL^2\kappa^2)\right]\end{aligned} \tag{26}$$

in which, $\Omega = GAL^2/(EI)$ and

$$\begin{pmatrix}\alpha_b\\ \beta_b\end{pmatrix} = \sqrt{\sqrt{\left[\kappa^2C_0^b(\Omega EI - P(L^2+\kappa^2\Omega))/2\right]^2 + P\Omega\kappa^2C_0^b} \pm \kappa^2C_0^b(\Omega EI - P(L^2+\kappa^2\Omega))/2} \tag{27}$$

Performing inverse Laplace transformation respect to s on Eqs. (25) and (26) as well as (21), one obtains

$$\begin{aligned}M(x) &= \sum_{i=1}^{8} C_iM_i^b(x)\\ V(x) &= \sum_{i=1}^{8} C_iV_i^b(x)\\ w(x) &= \sum_{i=1}^{8} C_iw_i^b(x)\\ \phi(x) &= \sum_{i=1}^{8} C_i\phi_i^b(x)\end{aligned} \tag{28}$$

in which, $m_i^b(x)$,$q_i^b(x)$,$w_i^b(x)$ and $\phi_i^b(x)$ are given in Appendix A.

From Table 1, the boundary conditions for elastic buckling analysis of a Timoshenko beam under simply supported boundary conditions are

$$w(0) = M(0) = 0 \tag{29}$$

$$w(L) = M(L) = 0 \tag{30}$$

Eqs. (22) and (29) requires

$$\begin{aligned}&C_1 = C_2\\ &C_5 = \left[EI\Omega C_3 + C_4(PL^2\kappa^2 2/c^2 - EI\Omega)\right]/(L^2\kappa^3) + C_8P\\ &C_6 = C_7 = 0\end{aligned} \tag{31}$$

Combination of Eqs. (28) with (30) gives

$$\begin{cases}C_2A_2^b(L) + C_3A_3^b(L) + C_4A_4^b(L) + C_8A_8^b(L) = 0\\ C_2B_2^b(L) + C_3B_3^b(L) + C_4B_4^b(L) + C_8B_8^b(L) = 0\end{cases} \tag{32}$$

in which, $\psi = w$ for $A^b = \Psi^b$, while $\psi = m$ for $B^b = \Psi^b$, and $\Psi^b$is defined as

$$\begin{aligned}
&\Psi_2^b(x) = \psi_1^b(x) + \psi_2^b(x)\\
&\Psi_3^b(x) = \psi_3^b(x) + EI\Omega\psi_5^b(x)/(L^2\kappa^3)\\
&\Psi_4^b(x) = \psi_4^b(x) + (pL^2\kappa^2 2 - c^2EI\Omega)\psi_5^b(x)/(c^2L^2\kappa^3)\\
&\Psi_8^b(x) = \psi\phi_5^b(x) + \psi_8^b(x)
\end{aligned} \tag{33}$$

Combination of Eqs. (23) and (28) with (31) gives

$$\begin{cases}
(F_2^b - 1)C_2 + F_3^bC_3 + F_4^bC_4 + F_8^bC_8 = 0\\
G_2^bC_2 + G_3^bC_3 + (G_4^b - 1)C_4 + G_8^bC_8 = 0
\end{cases} \tag{34}$$

where, $\psi = \phi'$ for $F^b = \Gamma^b$, while $\psi = \phi + w'$ for $G^b = \Gamma^b$, and Γ^b is defined as

$$\Gamma_i^b = \left[(\kappa^2 - c^2)\int_0^L \Psi_i^b(x)e^{-x/\kappa}\mathrm{d}x - \kappa c^2\Psi_i^b(L)\mathrm{e}^{-L/\kappa}\right]/2 \tag{35}$$

Therefore, combining Eqs. (32) and (34), one obtains

$$\begin{bmatrix}
A_2^b(L) & A_3^b(L) & A_4^b(L) & A_8^b(L)\\
B_2^b(L) & B_3^b(L) & B_4^b(L) & B_8^b(L)\\
F_2^b - 1 & F_3^b & F_4^b & F_8^b\\
G_2^b & G_3^b - 1 & G_4^b & G_8^b
\end{bmatrix}\begin{pmatrix} C_2\\ C_3\\ C_4\\ C_8\end{pmatrix} = 0 \tag{36}$$

Clearly, Eq. (36) is a set of homogeneous linear equations about C_i(i =2, 3, 4, 8) for elastic buckling of nonlocal strain gradient Timoshenko beam. The condition to obtain nonzero solution for Eq. (36) is that the coefficient matrix is singular, e.g.,

$$\det\begin{pmatrix}
A_2^b(L) & A_3^b(L) & A_4^b(L) & A_8^b(L)\\
B_2^b(L) & B_3^b(L) & B_4^b(L) & B_8^b(L)\\
F_2^b - 1 & F_3^b & F_4^b & F_8^b\\
G_2^b & G_3^b - 1 & G_4^b & G_8^b
\end{pmatrix} = 0 \tag{37}$$

Eq. (37) is a nonlinear characteristic equation from which one can determine the critical buckling load P. In this study, an approach combining Newton–Raphson iteration method and difference method is applied to solve the nonlinear Eq. (37).

Following similar procedure, one can obtain the nonlinear characteristic equations for buckling loads of nonlocal strain gradient Timoshenko beam subjected to other different boundary conditions.

4. Free vibration of nonlocal strain gradient Timoshenko beam

For free vibration problem of Timoshenko beam, it is assumed that

$$\begin{aligned}
&w(x,t) = W(x)\mathrm{e}^{i\omega t}\\
&\phi(x,t) = \Phi(x)\mathrm{e}^{i\omega t}\\
&M(x,t) = \hat{M}(x)\mathrm{e}^{i\omega t}\\
&V(x,t) = \hat{V}(x)\mathrm{e}^{i\omega t}
\end{aligned} \tag{38}$$

Substituting Eq. (38) into the differential governing Eq. (14) and neglecting the external force and performing Laplace transformation on them, one obtains

$$\begin{cases}
\mathcal{L}\{\hat{V}\} = (C_6 - m\omega^2\mathcal{L}\{W\})/s\\
\mathcal{L}\{\hat{M}\} = (C_6 + C_5s - m\omega^2\mathcal{L}\{W\})/s^2
\end{cases} \tag{39}$$

Combination of Eq. (21) with (38) and (39) gives

$$\begin{aligned}\mathcal{L}\{W\} &= \{s^5C_7c^2EI\kappa^2\Omega + s^4\kappa[C_6L^2\kappa^3 - EI\Omega(C_3+C_4+C_8c^2\kappa)]\\ &+s^3[EI(C_4-C_3+C_1\kappa+C_2\kappa-C_7\kappa^2)-C_5\kappa^4]-s^2[EI(C_2-C_1-C_8\kappa^2)\\ &+C_6\kappa^2(\kappa^2\Omega+L^2)]+(sC_5+C_6)\kappa^2\Omega\}/[EIc^2\kappa^2\Omega(s^2-\alpha_\nu^2)(s^2-\beta_\nu^2)(s^2-\gamma_\nu^2)]\\ \mathcal{L}\{\Phi\} &= \{s^7C_8c^4EI^2\kappa^2\Omega - s^6EI\kappa[(C_1+C_2)EI-C_3\kappa^3]+s^5c^2EI[\kappa^4(C_8m\omega^2L^2+C_6\Omega)\\ &-EI\Omega(C_1-C_2+2C_8\kappa^2)]+s^4\kappa[(C_2EI+C_1EI-C_5\kappa^3)(EI\Omega-2m\omega^2\kappa^2L^2)-EI\Omega c^2\kappa\\ &(C_5+m\omega^2\kappa^2C_7)]+s^3EI[(EI\Omega-m\omega^2\kappa^2L^2)(C_1-C_2+C_8\kappa^2)-C_6\kappa^2(\kappa^2+c^2)\\ &+m\omega^2\kappa^2((C_3+C_4)\kappa\Omega-C_8c^2L^2)]+s^2\kappa[C_5\kappa(EI\Omega-2m_0\omega^2\kappa^2L^2)+EIm\omega^2((C_1+C_2)L^2\\ &+\kappa\Omega(C_3-C_4+C_7(\kappa^2+c^2))\Omega)]+sEI[m\omega^2((C_1-C_2+C_8\kappa^2)L^2-\kappa\Omega(C_3+C_4)]+m\omega^2\\ &[C_5\kappa^2L^2-EI\Omega(C_3-C_4\kappa^2)]\}/[EI^2c^2\kappa^2\Omega(c^2s^2-1)(s^2-\alpha_\nu^2)(s^2-\beta_\nu^2)(s^2-\gamma_\nu^2)]\end{aligned} \tag{40}$$

in which,

$$\alpha_\nu = \sqrt{-\sqrt[3]{\frac{2b^3}{3\sqrt{12b^3+81d^2}-27d}}-\frac{a}{3}+\sqrt[3]{\frac{\sqrt{12b^3+81d^2}-9d}{18}}} \tag{41}$$

$$\beta_\nu = \sqrt{-\frac{(1+i\sqrt{3})b}{\sqrt[3]{12\sqrt{12b^3+81d^2}-108d}}-\frac{a}{3}+(1-i\sqrt{3})\sqrt[3]{\frac{\sqrt{12b^3+81d^2}-9d}{144}}} \tag{42}$$

$$\gamma_\nu = \sqrt{-\frac{(1-i\sqrt{3})b}{\sqrt[3]{12\sqrt{12b^3+81d^2}-108d}}-\frac{a}{3}+(1+i\sqrt{3})\sqrt[3]{\frac{\sqrt{12b^3+81d^2}-9d}{144}}} \tag{43}$$

where,

$$\begin{aligned}a &= (L^2m\omega^2\kappa^2-EI\Omega)/(c^2EI\Omega)\\ b &= -a^2/3-m\omega^2(L^2+\kappa^2\Omega)/(c^2EI\Omega)\\ d &= 2a^3/27+m\omega^2[3\Omega+a(L^2+\kappa^2\Omega)]/(3c^2EI\Omega)\end{aligned}$$

Performing inverse Laplace transformation on Eqs. (39) and (40), one gets

$$\begin{aligned}\hat{M}(x) &= \sum_{i=1}^{8}C_iM_i^\nu(x)\\ \hat{V}(x) &= \sum_{i=1}^{8}C_iV_i^\nu(x)\\ W(x) &= \sum_{i=1}^{8}C_iw_i^\nu(x)\\ \Phi(x) &= \sum_{i=1}^{8}C_i\phi_i^\nu(x)\end{aligned} \tag{44}$$

in which, $m_i^\nu(x)$,$q_i^\nu(x)$,$w_i^\nu(x)$ and $\phi_i^\nu(x)$ are given in Appendix B.

Similar to elastic bucking problem, the boundary conditions for free vibration analysis of Timoshenko beam under simply supported boundary conditions are

$$W(0) = \hat{M}(0) = 0 \tag{45}$$

$$W(L) = \hat{M}(L) = 0 \tag{46}$$

Eqs. (22) and (45) requires

$$\begin{aligned}C_1 &= C_2\\ C_3 &= C_4+C_6L^2\kappa^3/(EI\Omega)\\ C_5 &= C_7 = 0\end{aligned} \tag{47}$$

Combination of Eqs. (46) with (44) gives

$$\begin{cases}C_2A_2^\nu(x)+C_4A_4^\nu(x)+C_6A_6^\nu(x)+C_8A_8^\nu(x)=0\\ C_2B_2^\nu(x)+C_4B_4^\nu(x)+C_6B_6^\nu(x)+C_8B_8^\nu(x)=0\end{cases} \tag{48}$$

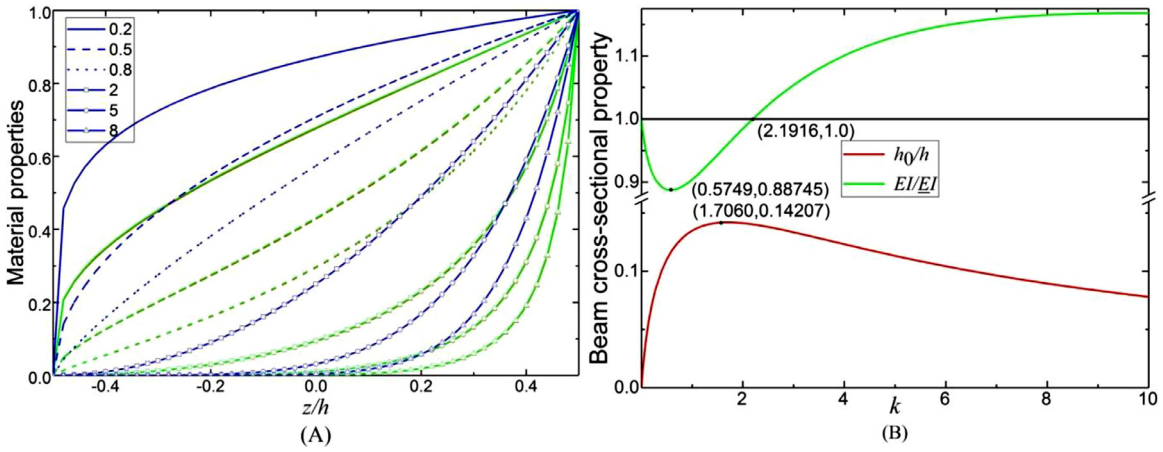

Fig. 2. Properties of FG beam: (A) ratios of effective Young's (blue line) and shear (green line) moduli and density (blue line) versus z under different k; (B) neutral position and bending stiffness.

in which, $\psi = W$ for $\Psi^v = A^v$, while $\psi = M$ for $\Psi^v = B^v$, and Ψ is defined as

$$\begin{aligned}
&\Psi_2^v(x) = \psi_1^v(x) + \psi_2^v(x)\\
&\Psi_4^v(x) = \psi_3^v(x) + \psi_4^v(x)\\
&\Psi_6^v(x) = \psi_6^b(x) + L^2\kappa^3\psi_3^b(x)/(EI\Omega)\\
&\Psi_8^v(x) = \psi_8^v(x)
\end{aligned} \tag{49}$$

Combination Eqs. (23) and (44) with (47) gives

$$\begin{cases}
(F_2^v - 1)C_2 + F_4^v C_4 + F_6^v C_6 + F_8^v C_8 = 0\\
G_2^v C_2 + (G_4^v - 1)C_4 + G_6^v C_6 + G_8^v C_8 = 0
\end{cases} \tag{50}$$

where, $\psi^v = \Phi'$ for $F^v = \Gamma^v$, while $\psi^v = \Phi + W'$ for $G^v = \Gamma^v$, and Γ^v is defined as

$$\Gamma_i^v = \left[(\kappa^2 - c^2)\int_0^L \Psi_i^v(x)\mathrm{e}^{-x/\kappa}\mathrm{d}x - \kappa c^2\Psi_i^v(L)\mathrm{e}^{-L/\kappa}\right]/2 \tag{51}$$

Similarly, from Eqs. (48) to (50), a nonlinear characteristic equation about ω can be derived and expressed for simply supported Timoshenko beam as

$$\det\begin{pmatrix}
A_2^v(L) & A_3^v(L) & A_4^v(L) & A_8^v(L)\\
B_2^v(L) & B_3^v(L) & B_4^v(L) & B_8^v(L)\\
F_2^v - 1 & F_3^v & F_4^v & F_8^v\\
G_2^v & G_3^v - 1 & G_4^v & G_8^v
\end{pmatrix} = 0 \tag{52}$$

Following a similar procedure, one can obtain the nonlinear characteristic equations for free vibration of nonlocal strain gradient Timoshenko beam subjected to other boundary conditions.

5. Numerical study and discussion

In this subsection, the influence of material length scale parameters κ and c on the elastic buckling load and free vibration frequency of nonlocal gradient FG Timoshenko beam is studied. The FG beam is assumed to be composed of aluminum ($E_a = 70\mathrm{GPa}, \rho_a = 2700\mathrm{kg/m^3}$, $\upsilon_a = 0.23$) and ceramic ($E_c = 380\mathrm{GPa}, \rho_c = 3800\mathrm{kg/m^3}$, $\upsilon_c = 0.23$) [52]. In this study, $\mathrm{k_s} = 5/6$ is adopted for rectangular cross-section of beam.

Fig. 2(A) shows the ratios of effective material properties versus z under different FG exponent index k, in which red, green and blue lines represent ratios of effective Young's modulus$((\mathrm{E_e} - \mathrm{E_a})/(\mathrm{E_c} - \mathrm{E_a}))$ and shear modulus $((\mathrm{G_e} - \mathrm{G_a})/(\mathrm{G_c} - \mathrm{G_a}))$ as well as density$((\rho_\mathrm{e} - \rho_\mathrm{a})/(\rho_\mathrm{c} - \rho_\mathrm{a}))$, respectively. Fig. 2(A) shows that the ratios for effective Young's and shear moduli follow almost same distribution law. In addition, the ratio for effective Young's and shear moduli as well density increase with the increase of z. Fig. 2(B) illustrates the influence of exponent index on beam cross-sectional properties, in which $\underline{E}I$ represents the bending stiffness due to homogeneous material with same volume fraction for both aluminum and ceramic, e.g.,

$$\underline{E}I = \underline{E}\int_A z^2\mathrm{d}A \tag{53}$$

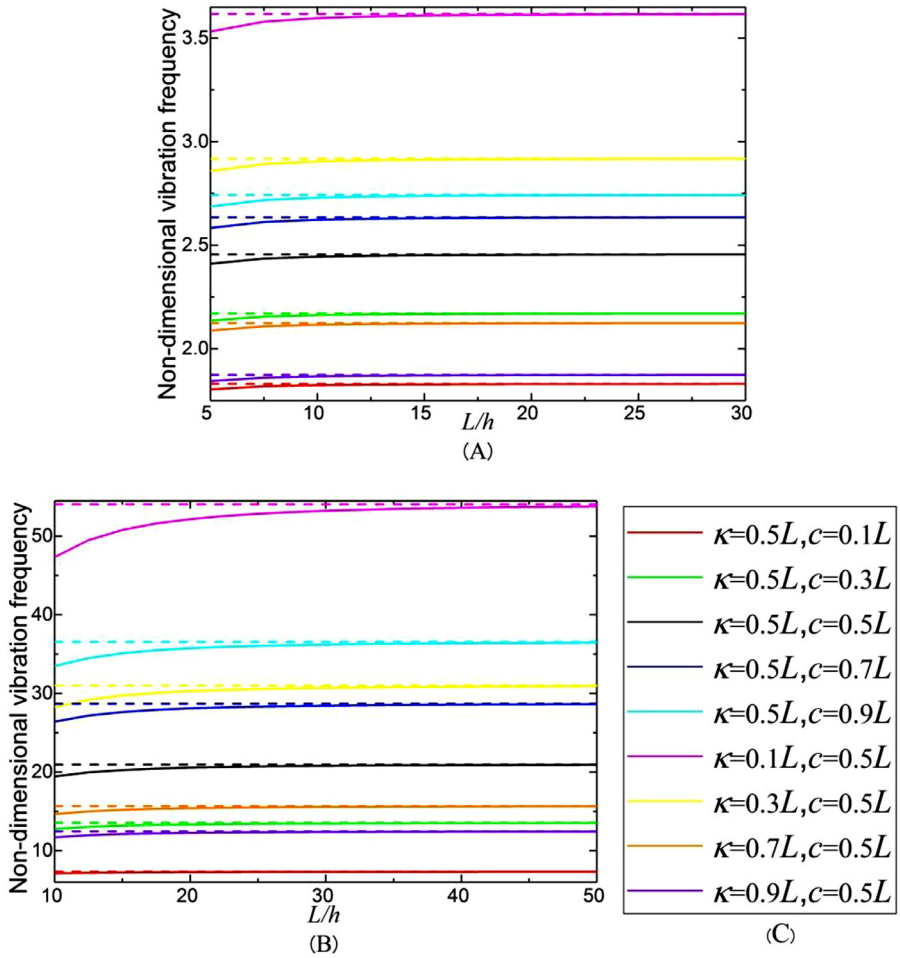

Fig. 3. Comparison of non-dimensional vibration frequency of (A) CF- and (B) CC- Timoshenko (solid lines) and Euler–Bernoulli (dash lines) beams under different L/h and (C) legend for (A) and (B).

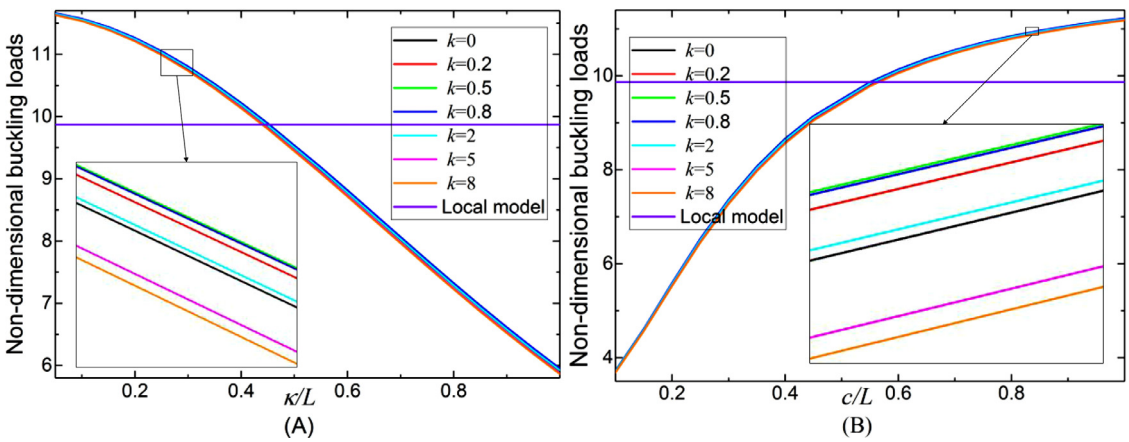

Fig. 4. Non-dimensional buckling loads versus (A) κ/L for $c/L = 0.5$ and (B) c/L for $\kappa/L = 0.5$ under different exponent index k.

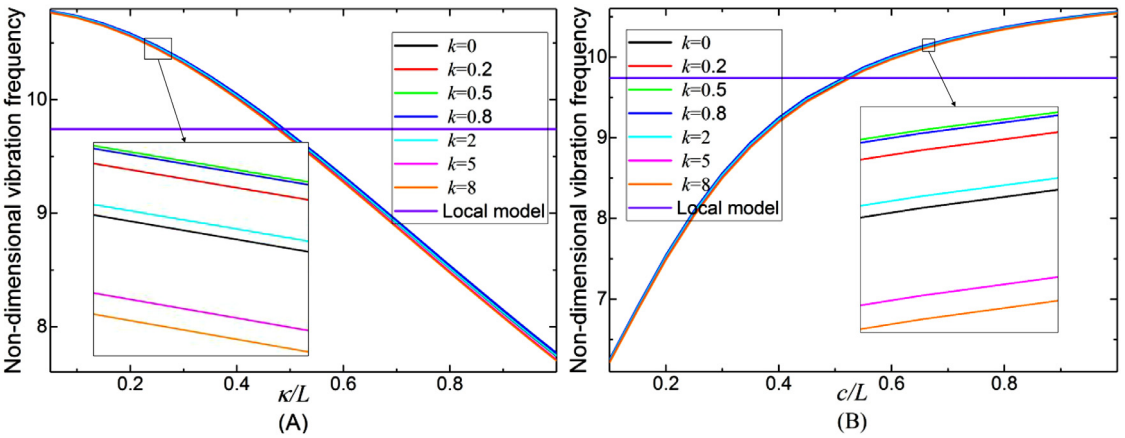

Fig. 5. Non-dimensional vibration frequencies versus (A) κ/L for $c/L = 0.5$ and (B) c/L for $\kappa/L = 0.5$under different exponent index k.

It can be seen from Fig. 2(B) that $EI\ /\underline{EI}$ decreases from 1 to 0.88745 with the increase of k from 0 to 0.5749, and then increases consistently with the further increase of k, which agree well with the results in Li et al. [44], in which rule-of-mixture is applied to estimate the Young's modulus of FG Euler–Bernoulli beam. Meanwhile, one can notice that $EI\ /\underline{EI}$ equals to 1 for k=2.1916. In addition, Fig. 2(B) shows that the h_0/h increases with the increase of k from 0 to 1.7060, and then decreases consistently with the further increase of k.

Fig. 3 illustrates the influence of L/h on the non-dimensional vibration frequency of CF- and CC- Timoshenko beams made of pure aluminum for different κ/L and c/L, in which the non-dimensional vibration frequencyϖ is defined as

$$\varpi = \omega L^2\sqrt{m_0/(EI)} \tag{54}$$

Meanwhile, the non-dimensional vibration frequencies of Euler–Bernoulli beam from Apuzzo et al. [53] are plotted for comparison. Fig. 3 shows that the vibration frequency of Timoshenko beam is less than corresponding Euler–Bernoulli beam. This can be explained by that the stiffness of Timoshenko beam is less than corresponding Euler–Bernoulli beam due to the existence of shear deformation in Timoshenko beam. Meanwhile, with the increase of L/h, the vibration frequencies of Timoshenko beam increase and approach to those of Euler–Bernoulli beam because the effect of shear deformation in Timoshenko beam decrease with the increase of L/h.

Figs. 4 and 5 illustrate the influence of exponent index k on the curves of 1st-order non-dimensional buckling loads and vibration frequencies of SS Timoshenko beams (L/h=10) versus κ/L and c/L, respectively, in which the non-dimensional buckling load P is defined as

$$\bar{P} = PAL^2/(EI) \tag{55}$$

Figs. 4 and 5 show that the influence of exponent index k on non-dimensional buckling loads and vibration frequencies is not significant for different structural length-scale parameters. Meanwhile, the non-dimensional buckling loads and vibration frequencies of FG-beam are bigger and smaller than those of homogeneous beam for k<=2 and k>5, respectively. In addition, the non-dimensional buckling loads and vibration frequencies increase with the increase of k from 0. to 0.5, and then decrease with the increase of k from 0.8 to 8, which is opposite to the distribution for bending stiffness as shown in Fig. 2(B). It can be explained by that EI is denominator for both non-dimensional buckling loads (Eq. (55)) and vibration frequencies (Eq. (54)).

Figs. 6 and 7 show clearly that under different boundary conditions, the 1st-order non-dimensional buckling load and vibration frequency of nonlocal homogeneous Timoshenko beams decrease consistently with the increase of κ/L, while increase consistently with the increase of c/L. Meanwhile, it is interesting to find that the buckling loads of CF-Timoshenko beams are exactly same as those of SG-Timoshenko beams. In addition, the 1st-order non-dimensional buckling load and vibration frequency of nonlocal strain gradient Timoshenko beams increase with the increase of L/h, which agrees with the result shown in Fig. 3. However, the influence of L/h on the 1st-order non-dimensional buckling load and vibration frequency decrease with the increase of κ/L for nonlocal strain gradient Timoshenko beam. Compared the results from local model, both softening and toughening effects (below and above black lines) can be observed.

Fig. 8 illustrates the boundaries between the softening and toughening regions for the 1st-order buckling load and vibration frequency of nonlocal strain gradient Timoshenko beams, in which the regions below the curves are the toughening regions. It can be seen from Fig. 8 that the toughening regions increase with the increase of L/h from 10 to 15, except that the boundaries between softening and toughening regions for buckling load of SS-beam as well as vibration frequencies of CC-, SC, SS- and CG-beams, which are almost independent on the value of L/h. Meanwhile, the toughening regions for buckling loads grow larger and larger from CF- and SG-, CG-, SS-, CC- and SC-beams, while the toughening regions for vibration

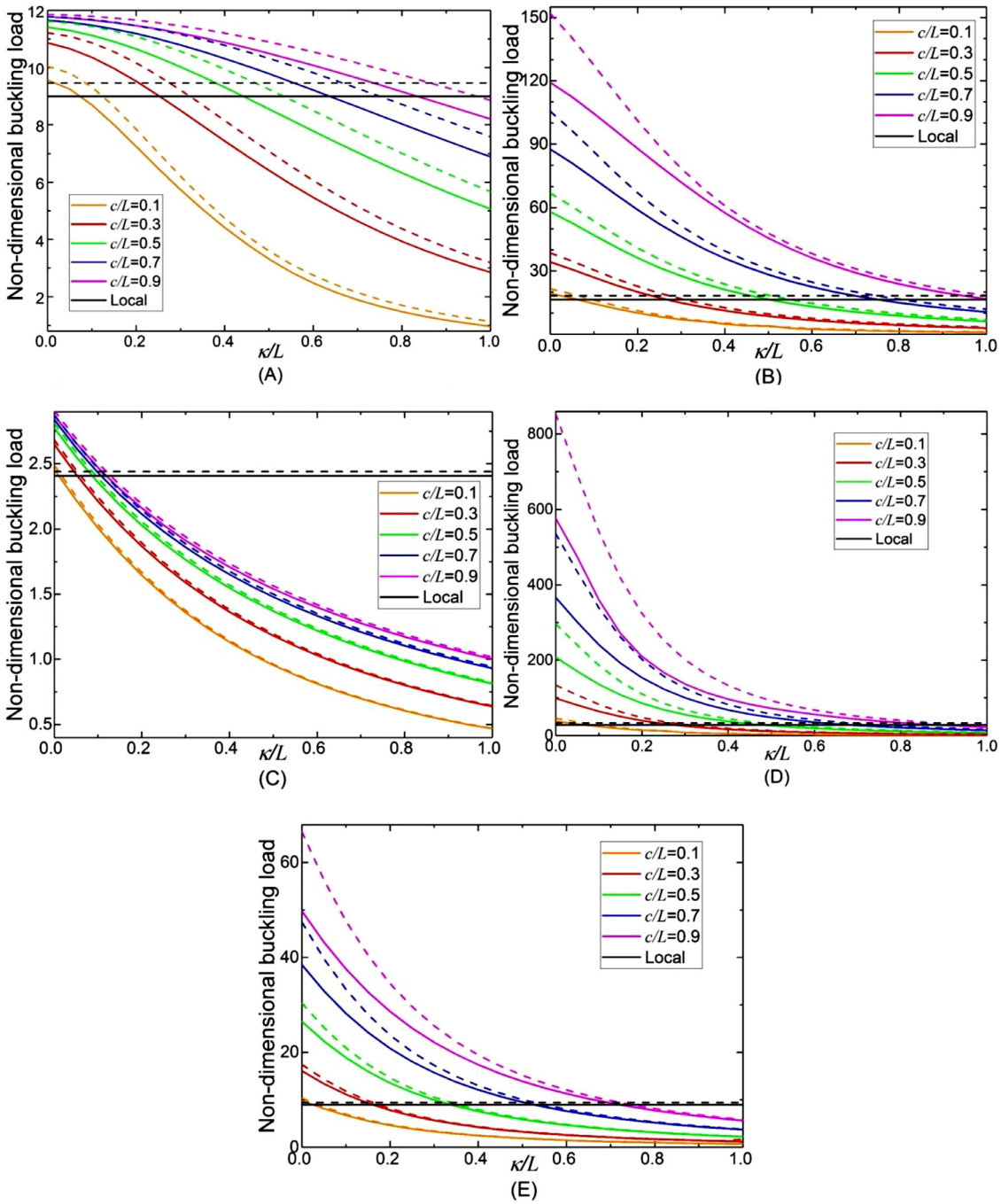

Fig. 6. Non-dimensional buckling loads of (A) SS-, (B) CS-, (C) SG&CF-, (D) CC- and (E) CG-Timoshenko beam made of homogeneous material versus κ/L for different c/L(solid and dash lines indicate L =10h and L =15h, respectively).

frequencies grow larger and larger from SG-, CF-, CG-, CC-, SS- and SC-beams. In addition, it can be observed from Fig. 8 that the softening effects dominate the buckling and vibration response of nonlocal strain gradient Timoshenko beams except for vibration response of SC-Timoshenko beam. Furthermore, it should be noticed that all the boundary lines in Fig. 8 pass through (0,0) which indicates that the Timoshenko beam based on nonlocal strain gradient integral model can be recovered when both κ and c approach to 0.

Figs. 9 and 10 illustrate the influence of κ/L and c/L on the high-order normalized buckling loads (NBLs) and vibration frequencies (NVFs) of nonlocal strain gradient Timoshenko beams under different boundary conditions for c/L =0.5 and κ/L =0.5, respectively, in which NBL and NVF are defined as ratio between nonlocal model and local models. Similar to the 1st-

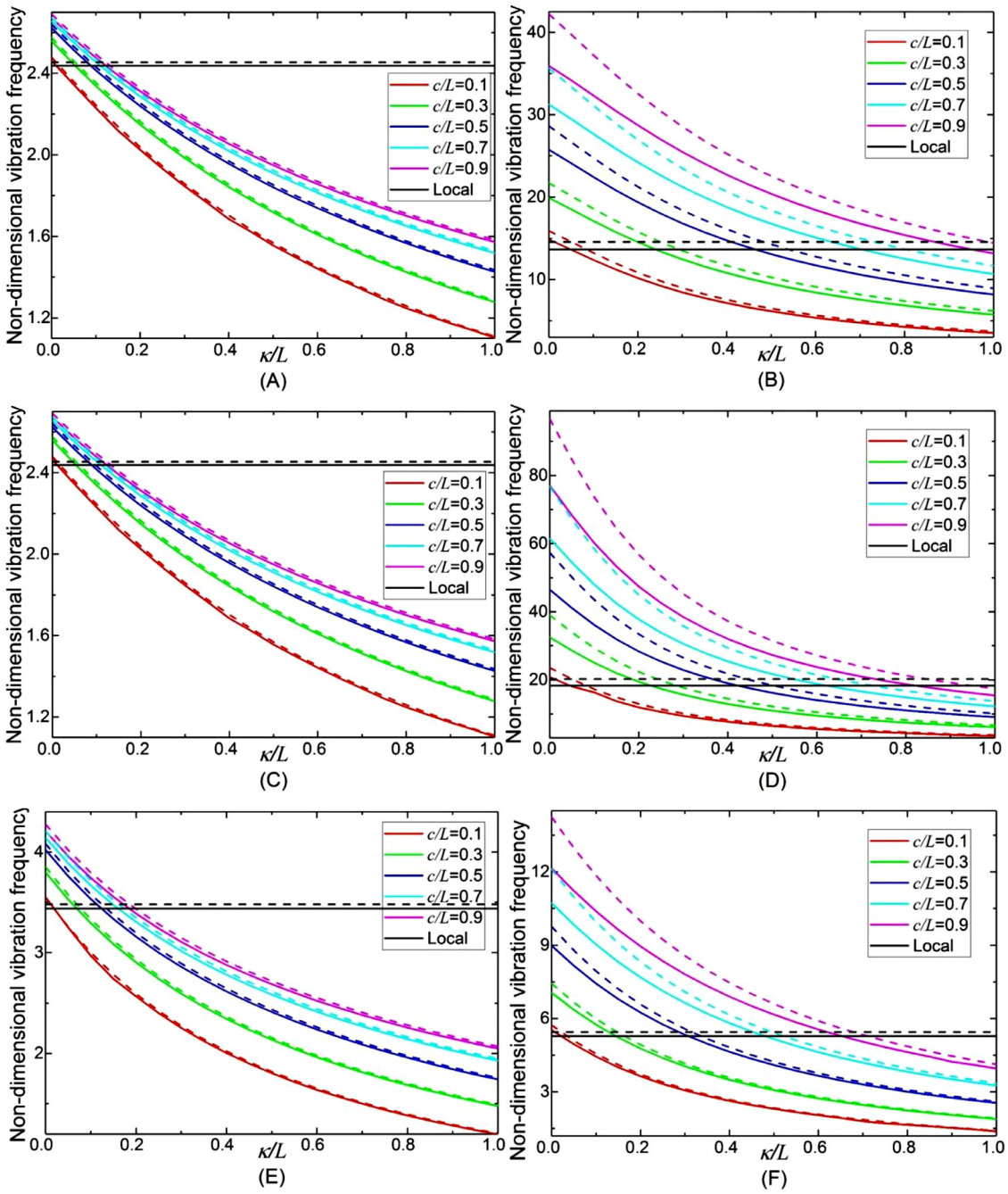

Fig. 7. Non-dimensional vibration frequencies of (A) SS-, (B) CS-, (C) SG-, (D) CC-, (E) CG- and CF-Timoshenko beams made of homogeneous material versus κ/L for different c/L(solid and dash lines indicate L =10h and L =15h, respectively).

order buckling load and vibration frequency, the high-order NBLs and NVFs of nonlocal strain gradient Timoshenko beams decreases with the increase of κ/L for c/L =0.5, while increase with the increase of c/L for κ/L =0.5. Meanwhile, with the increase of buckling and vibration order, the buckling loads and vibration frequencies increase and decrease in low-value and high-value of κ/L forc/L =0.5, respectively, while decrease and increase in low-value and high-value of c/L for κ/L =0.5.

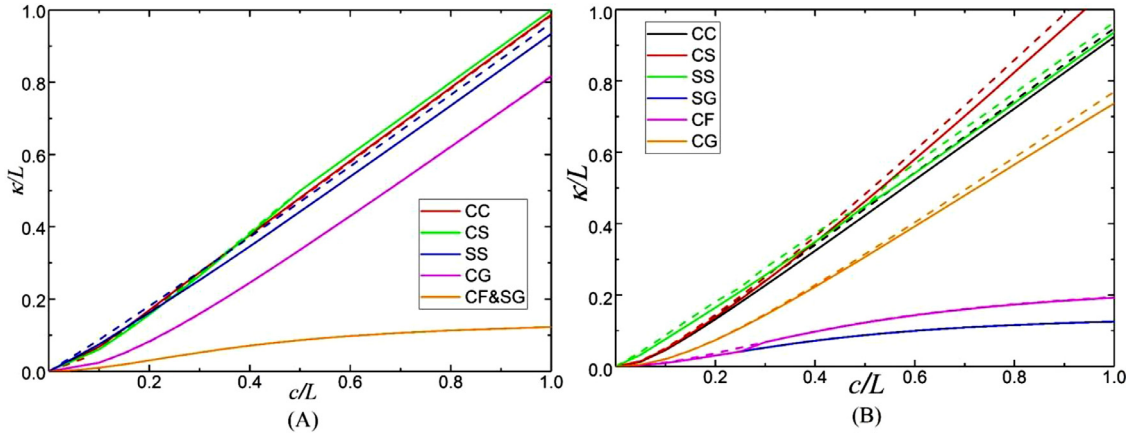

Fig. 8. Boundary between softening and toughening regions for 1st order (A) buckling load and (B) vibration frequency of nonlocal strain gradient Timoshenko beams made of homogeneous material (solid and dash lines indicate L =10h and L =15h, respectively).

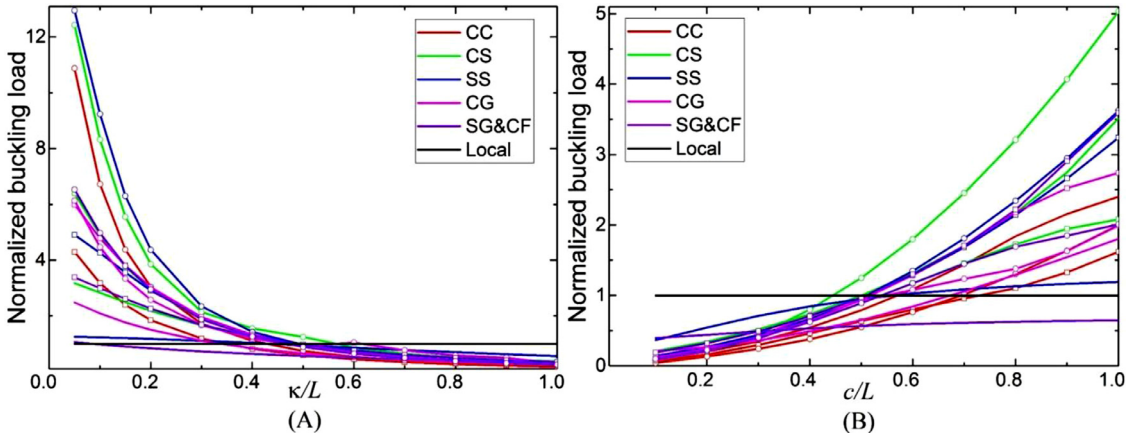

Fig. 9. The influence of (A) κ/L and (B) c/L on high-order NBLs of Timoshenko beams made of homogeneous material under different boundary conditions for c/L =0.5 and κ/L =0.5, respectively (solid, square- and circular-scatter lines indicate 1st, 2nd and 3rd NBLs).

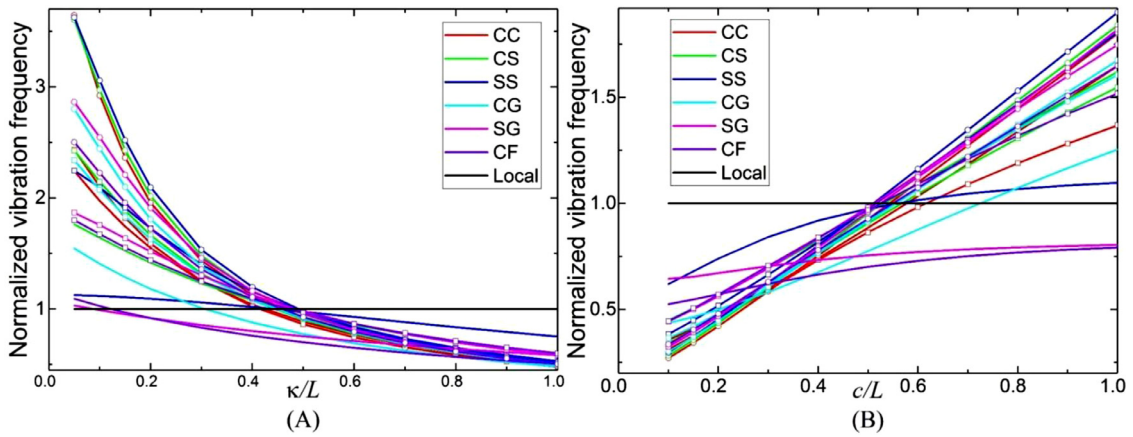

Fig. 10. The influence of (A) κ/L and (B) c/L on high-order NVFs of Timoshenko beams made of homogeneous material under different boundary conditions for c/L =0.5 and κ/L =0.5, respectively (solid, square- and circular-scatter lines indicate 1st, 2nd and 3rd NVFs).

6. Conclusions

In this paper, nonlocal strain gradient integral model is applied to analyze the elastic buckling and vibration of functionally graded Timoshenko beam under different boundary conditions. The Laplace transform technique is applied to solve the integro-differential equations directly, and the bending deflections and moments, as well as cross-sectional rotation and shear force are derived and expressed explicitly with eight unknown constants. The nonlinear characteristic equations about buckling load and vibration frequency can be derived explicitly for different boundary conditions and constitutive constraints. The numerical analysis is performed to study the influence of FG exponent index, length-scale parameters, boundary conditions, ratio between length and thickness as well as buckling and vibration orders on the buckling load and vibration frequency, and several conclusions can be summarized as following:

1. The influence of exponent index on non-dimensional buckling loads and vibration frequencies is not significant under different structural length-scale parameters.
2. Buckling loads and vibration frequencies of nonlocal strain gradient Timoshenko beams increase consistently the increase of c/L and the decrease ofκ/L.
3. The influence of L/h on the 1st-order non-dimensional buckling load and vibration frequency decrease with the increase of κ/L for nonlocal strain gradient Timoshenko beam.
4. Softening effect dominates the size-dependent response of Timoshenko beam. The toughening regions for buckling loads grow larger and larger from CF- and SG-, CG-, SS-, CC- and SC-beams, while the toughening regions for vibration frequencies grow larger and larger from SG-, CF-, CG-, CC-, SS- and SC-beams.
5. The effects of material length-scale parameters on buckling loads and vibration frequencies increase with the increase of buckling and vibration order.

Acknowledgments

The work is supported by the National Natural Science Foundation of China (No. 11672131) and the Priority Academic Program Development of Jiangsu Higher Education Institutions.

Appendix A. List of Laplace transformation for buckling analysis

A.1. Coefficient functions for bending moment

$$M_1^b(x)= P\Omega EI(\kappa W_3^b(x) + W_2^b(x))C_0^b \tag{A.1}$$

$$M_2^b(x)= P\Omega EI(\kappa W_3^b(x) - W_2^b(x))C_0^b \tag{A.2}$$

$$M_3^b(x)= - P\Omega EI(W_3^b(x) + \kappa W_4^b(x))C_0^b \tag{A.3}$$

$$M_4^b(x)= P\Omega EI(W_3^b(x) - \kappa W_4^b(x))C_0^b \tag{A.4}$$

$$M_5^b(x)=\Omega EI\kappa^2(c^2W_4^b(x) - W_2^b(x))C_0^b \tag{A.5}$$

$$M_6^b(x)= W_5^b(x) + \kappa^2 W_3^b(x)(PL^2 - \Omega EI)C_0^b \tag{A.6}$$

$$M_7^b(x)= P\left[W_5^b(x) + \kappa^2 W_3^b(x)(pL^2 - \Omega EI)C_0^b\right] \tag{A.7}$$

$$M_8^b(x)= P\kappa^2 EI(W_2^b(x) - c^2 W_4^b(x))\Omega C_0^b \tag{A.8}$$

in which, $C_0^b= 1/(\kappa^2c^2EI\Omega - pL^2\kappa^4)$, and

$$W_0^b(x)=\mathcal{L}\left\{\frac{s^0}{s^2(s^2-\alpha_b^2)(s^2+\beta_b^2)}\right\} = \frac{\alpha_b^3\sin(\beta_b x) + \beta_b^3 sh(\alpha_b x)}{\alpha_b^3\beta_b^3(\alpha_b^2+\beta_b^2)} - \frac{x}{\alpha_b^2\beta_b^2} \tag{A.9}$$

$$W_1^b(x)=\mathcal{L}\left\{\frac{s^1}{s^2(s^2-\alpha_b^2)(s^2+\beta_b^2)}\right\} = \frac{1}{\alpha_b^2\beta_b^2} - \frac{\alpha_b^2\cos(\beta_b x) + \beta_b^2 ch(\alpha_b x)}{\alpha_b^2\beta_b^2(\alpha_b^2+\beta_b^2)} \tag{A.10}$$

$$W_2^b(x)=\mathcal{L}\left\{\frac{s^2}{s^2(s^2-\alpha_b^2)(s^2+\beta_b^2)}\right\}=\frac{\beta_b sh(\alpha_b x)-\alpha_b\sin(\beta_b x)}{\alpha_b\beta_b(\alpha_b^2+\beta_b^2)} \tag{A.11}$$

$$W_3^b(x)=\mathcal{L}\left\{\frac{s^3}{s^2(s^2-\alpha_b^2)(s^2+\beta_b^2)}\right\}=\frac{ch(\alpha_b x)-\cos(\beta_b x)}{\alpha_b^2+\beta_b^2} \tag{A.12}$$

$$W_4^b(x)=\mathcal{L}\left\{\frac{s^4}{s^2(s^2-\alpha_b^2)(s^2+\beta_b^2)}\right\}=\frac{\beta_b\sin(\beta_b x)+\alpha_b sh(\alpha_b x)}{\alpha_b^2+\beta_b^2} \tag{A.13}$$

$$W_5^b(x)=\mathcal{L}\left\{\frac{s^5}{s^2(s^2-\alpha_b^2)(s^2+\beta_b^2)}\right\}=\frac{\alpha_b^2 ch(\alpha_b x)+\beta_b^2\cos(\beta_b x)}{\alpha_b^2+\beta_b^2} \tag{A.14}$$

A.2. Coefficient functions for shear force

$$V_1^b(x)=P\Omega EI(\kappa W_4^b(x)+W_3^b(x))C_0^b \tag{A.15}$$

$$V_2^b(x)=P\Omega EI(\kappa W_4^b(x)-W_3^b(x))C_0^b \tag{A.16}$$

$$V_3^b(x)=-P\Omega EI(W_4^b(x)+\kappa W_5^b(x))C_0^b \tag{A.17}$$

$$V_4^b(x)=P\Omega EI(W_4^b(x)-\kappa W_5^b(x))C_0^b \tag{A.18}$$

$$V_5^b(x)=\Omega EI\kappa^2(c^2W_5^b(x)-W_3^b(x))C_0^b \tag{A.19}$$

$$V_6^b(x)=P\kappa^2(W_2^b(x)-\kappa^2W_4^b(x))\Omega C_0^b \tag{A.20}$$

$$V_7^b(x)=P^2\kappa^2(W_2^b(x)-\kappa^2W_4^b(x))\Omega C_0^b \tag{A.21}$$

$$V_8^b(x)=P\kappa^2EI(W_3^b(x)-c^2W_5^b(x))\Omega C_0^b \tag{A.22}$$

A.3. Coefficient functions for bending deflection

$$w_1^b(x)=\Omega EI(\kappa W_3^b(x)+W_2^b(x))C_0^b \tag{A.23}$$

$$w_2^b(x)=\Omega EI(\kappa W_3^b(x)-W_2^b(x))C_0^b \tag{A.24}$$

$$w_3^b(x)=-\Omega EI(W_3^b(x)+\kappa W_4^b(x))C_0^b \tag{A.25}$$

$$w_4^b(x)=\Omega EI(W_3^b(x)-\kappa W_4^b(x))C_0^b \tag{A.26}$$

$$w_5^b(x)=\kappa^2\left[\Omega(W_0^b(x)-\kappa^2W_2^b(x))-L^2(W_2^b(x)-\kappa^2W_4^b(x))\right]C_0^b \tag{A.27}$$

$$w_6^b(x)=\kappa^2(W_1^b(x)-\kappa^2W_3^b(x))\Omega C_0^b \tag{A.28}$$

$$w_7^b(x)=W_5^b(x)+\kappa^2W_2^b(x)(pL^2-EI\Omega)C_0^b \tag{A.29}$$

$$w_8^b(x)=\kappa^2EI(W_2^b(x)-c^2W_4^b(x))\Omega C_0^b \tag{A.30}$$

A.4. Coefficient functions for cross-sectional rotation

$$\phi_1^b(x)=(\Omega EI-PL^2)(\Phi_2^b(x)+\kappa\Phi_3^b(x))C_0^b-(\Phi_4^b(x)+\kappa\Phi_5^b(x))/\kappa^2 \tag{A.31}$$

$$\phi_2^b(x)=(\Omega EI-PL^2)(\kappa\Phi_3^b(x)-\Phi_2^b(x))C_0^b+(\Phi_4^b(x)-\kappa\Phi_5^b(x))/\kappa^2 \tag{A.32}$$

$$\phi_3^b(x)=P\Omega\left[\Phi_1^b(x)+\kappa\Phi_2^b(x)-\kappa^2(\Phi_3^b(x)+\kappa\Phi_4^b(x))\right]C_0^b \tag{A.33}$$

$$\phi_4^b(x)=P\Omega\left[\kappa\Phi_2^b(x)-\Phi_1^b(x)+\kappa^2(\Phi_3^b(x)-\kappa\Phi_4^b(x))\right]C_0^b \tag{A.34}$$

$$\phi_5^b(x)=\Omega\kappa^2\left[\Phi_0^b(x)-\kappa^2\Phi_2^b(x)-c^2(\Phi_2^b(x)-\kappa^2\Phi_4^b(x))\right]C_0^b \tag{A.35}$$

$$\phi_6^b(x)=\left[(EI\Omega-PL^2)(\Phi_1^b(x)-\kappa^2\Phi_3^b(x))C_0^b-\Phi_3^b(x)+\kappa^2\Phi_5^b(x)\right]/EI \tag{A.36}$$

$$\phi_7^b(x)=P\phi_6^b(x) \tag{A.37}$$

$$\phi_8^b(x)=(EI\Omega-PL^2)(\Phi_2^b(x)-c^2\Phi_4^b(x))C_0^b-\Phi_4^b(x)+c^2\Phi_6^b(x) \tag{A.38}$$

in which,

$$\begin{aligned}&\Phi_0^b(x)=\mathcal{L}\left\{\left[s\left(c^2s^2-1\right)\left(s^2-\alpha_b^2\right)(s^2+\beta_b^2)\right]^{-1}\right\}=1/\alpha_b^2\beta_b^2+\\&\left[\beta_b^2(c^2\beta_b^2+1)ch(\alpha_bx)-\alpha_b^2\beta_b^2c^4(\alpha_b^2+\beta_b^2)ch(x/c)-\right.\\&\left.\alpha_b^2\left(c^2\alpha_b^2-1\right)cos(\beta_bx)\right]/\left[\alpha_b^2\beta_b^2\left(\alpha_b^2+\beta_b^2\right)\left(c^2\alpha_b^2-1\right)\left(c^2\beta_b^2+1\right)\right]\end{aligned} \tag{A.39}$$

$$\begin{aligned}\Phi_1^b(x)&=\mathcal{L}\{\left[(c^2s^2-1)(s^2-\alpha_b^2)(s^2+\beta_b^2)\right]^{-1}\}=[\alpha_b(c^2\alpha_b^2-1)\sin(\beta_bx)\\&+\left[\beta_b(c^2\beta_b^2+1)sh(\alpha_bx)-c^3\alpha_b\beta_b(\alpha_b^2+\beta_b^2)sh(x/c)\right]\\&/\left[\alpha_b\beta_b(\alpha_b^2+\beta_b^2)(c^2\alpha_b^2-1)(c^2\beta_b^2+1)\right]\end{aligned} \tag{A.40}$$

$$\begin{aligned}\Phi_2^b(x)&=\mathcal{L}\{s\left[(c^2s^2-1)(s^2-\alpha_b^2)(s^2+\beta_b^2)\right]^{-1}\}=\left[(c^2\beta_b^2+1)ch(\alpha_bx)\right.\\&\left.-c^2(\alpha_b^2+\beta_b^2)ch(x/c)-(c^2\alpha_b^2-1)cos(\beta_bx)\right]/\left[(\alpha_b^2+\beta_b^2)(c^2\alpha_b^2-1)(c^2\beta_b^2+1)\right]\end{aligned} \tag{A.41}$$

$$\begin{aligned}\Phi_3^b(x)&=\mathcal{L}\{s^2\left[(c^2s^2-1)(s^2-\alpha_b^2)(s^2+\beta_b^2)\right]^{-1}\}=\left[\alpha_b(c^2\beta_b^2+1)sh(\alpha_bx)\right.\\&\left.-c(\alpha_b^2+\beta_b^2)sh(x/c)-\beta_b(c^2\alpha_b^2-1)\sin(\beta_bx)\right]/\left[(\alpha_b^2+\beta_b^2)(c^2\alpha_b^2-1)(c^2\beta_b^2+1)\right]\end{aligned} \tag{A.42}$$

$$\begin{aligned}\Phi_4^b(x)&=\mathcal{L}\{s^3\left[(c^2s^2-1)(s^2-\alpha_b^2)(s^2+\beta_b^2)\right]^{-1}\}=\left[\alpha_b^2(c^2\beta_b^2+1)ch(\alpha_bx)\right.\\&\left.-(\alpha_b^2+\beta_b^2)ch(x/c)-(c^2\alpha_b^2-1)\beta_b^2\sin(\beta_bx)\right]/\left[(\alpha_b^2+\beta_b^2)(c^2\alpha_b^2-1)(c^2\beta_b^2+1)\right]\end{aligned} \tag{A.43}$$

$$\begin{aligned}\Phi_5^b(x)&=\mathcal{L}\{s^4\left[(c^2s^2-1)(s^2-\alpha_b^2)(s^2+\beta_b^2)\right]^{-1}\}=\left[c\alpha_b^3(c^2\beta_b^2+1)sh(\alpha_bx)\right.\\&\left.-(\alpha_b^2+\beta_b^2)sh(x/c)+c\beta_b^3(c^2\alpha_b^2-1)\sin(\beta_bx)\right]/\left[c(\alpha_b^2+\beta_b^2)(c^2\alpha_b^2-1)(c^2\beta_b^2+1)\right]\end{aligned} \tag{A.44}$$

$$\begin{aligned}\Phi_6^b(x)&=\mathcal{L}\{s^5\left[(c^2s^2-1)(s^2-\alpha_b^2)(s^2+\beta_b^2)\right]^{-1}\}=\left[c^2\alpha_b^4(c^2\beta_b^2+1)ch(\alpha_bx)\right.\\&\left.-(\alpha_b^2+\beta_b^2)ch(x/c)-c^2(c^2\alpha_b^2-1)\beta_b^4\cos(\beta_bx)\right]/\left[c^2(\alpha_b^2+\beta_b^2)(c^2\alpha_b^2-1)(c^2\beta_b^2+1)\right]\end{aligned} \tag{A.45}$$

Appendix B. List of Laplace transformation for free vibration analysis

B.1. Coefficient functions for bending moment

$$M_1^v(x) = -m\omega^2(W_0^v(x) + \kappa W_1^v(x))/(c^2\kappa^2) \tag{B.1}$$

$$M_2^v(x) = m\omega^2(W_0^v(x) - \kappa W_1^v(x))/(c^2\kappa^2) \tag{B.2}$$

$$M_3^v(x) = m\omega^2(W_1^v(x) + \kappa W_2^v(x))/(c^2\kappa^2) \tag{B.3}$$

$$M_4^v(x) = m\omega^2(\kappa W_2^v(x) - W_1^v(x))/(c^2\kappa^2) \tag{B.4}$$

$$M_5^v(x) = \left[m\omega^2L^2(\kappa^2 W_3^v(x) - W_2^v(x)) + EI(c^2 W_5^v(x) - W_3^v(x))\right]/(c^2EI\Omega) \tag{B.5}$$

$$M_6^v(x) = W_4^v(x) - W_2^v(x)/c^2 \tag{B.6}$$

$$M_7^v(x) = m\omega^2(W_1^v(x) - c^2 W_3^v(x))/c^2 \tag{B.7}$$

$$M_8^v(x) = m\omega^2(W_2^v(x) - W_0^v(x)/c^2) \tag{B.8}$$

in which,

$$\begin{aligned} W_0^v(x) = \mathcal{L}\{&\left[(s^2-\gamma_v^2)(s^2-\alpha_v^2)(s^2-\beta_v^2)\right]^{-1}\} = \left[\beta_v\gamma_v(\beta_v^2-\gamma_v^2)sh(\alpha_v x)\right. \\ &\left.+\alpha_v\gamma_v(\gamma_v^2-\alpha_v^2)sh(\beta_v x) + \alpha_v\beta_v(\alpha_v^2-\beta_v^2)sh(\gamma_v x)\right]/\left[\alpha_v\beta_v\gamma_v(\alpha_v^2-\beta_v^2)(\alpha_v^2-\gamma_v^2)(\beta_v^2-\gamma_v^2)\right] \end{aligned} \tag{B.9}$$

$$\begin{aligned} W_1^v(x) = \mathcal{L}\{&s\left[(s^2-\gamma_v^2)(s^2-\alpha_v^2)(s^2-\beta_v^2)\right]^{-1}\} = \left[(\beta_v^2-\gamma_v^2)ch(\alpha_v x)\right. \\ &\left.+(\gamma_v^2-\alpha_v^2)ch(\beta_v x) + (\alpha_v^2-\beta_v^2)ch(\gamma_v x)\right]/\left[(\alpha_v^2-\beta_v^2)(\alpha_v^2-\gamma_v^2)(\beta_v^2-\gamma_v^2)\right] \end{aligned} \tag{B.10}$$

$$\begin{aligned} W_2^v(x) = \mathcal{L}\{&s^2\left[(s^2-\gamma_v^2)(s^2-\alpha_v^2)(s^2-\beta_v^2)\right]^{-1}\} = \left[\alpha_v(\beta_v^2-\gamma_v^2)sh(\alpha_v x)\right. \\ &\left.+\beta_v(\gamma_v^2-\alpha_v^2)sh(\beta_v x) + \gamma_v(\alpha_v^2-\beta_v^2)sh(\gamma_v x)\right]/\left[(\alpha_v^2-\beta_v^2)(\alpha_v^2-\gamma_v^2)(\beta_v^2-\gamma_v^2)\right] \end{aligned} \tag{B.11}$$

$$\begin{aligned} W_3^v(x) = \mathcal{L}\{&s^3\left[(s^2-\gamma_v^2)(s^2-\alpha_v^2)(s^2-\beta_v^2)\right]^{-1}\} = \left[\alpha_v^2(\beta_v^2-\gamma_v^2)ch(\alpha_v x)\right. \\ &\left.+\beta_v^2(\gamma_v^2-\alpha_v^2)ch(\beta_v x) + \gamma_v^2(\alpha_v^2-\beta_v^2)ch(\gamma_v x)\right]/\left[(\alpha_v^2-\beta_v^2)(\alpha_v^2-\gamma_v^2)(\beta_v^2-\gamma_v^2)\right] \end{aligned} \tag{B.12}$$

$$\begin{aligned} W_4^v(x) = \mathcal{L}\{&s^4\left[(s^2-\gamma_v^2)(s^2-\alpha_v^2)(s^2-\beta_v^2)\right]^{-1}\} = \left[\alpha_v^3(\beta_v^2-\gamma_v^2)sh(\alpha_v x)\right. \\ &\left.+\beta_v^3(\gamma_v^2-\alpha_v^2)sh(\beta_v x) + \gamma_v^3(\alpha_v^2-\beta_v^2)sh(\gamma_v x)\right]/\left[(\alpha_v^2-\beta_v^2)(\alpha_v^2-\gamma_v^2)(\beta_v^2-\gamma_v^2)\right] \end{aligned} \tag{B.13}$$

$$\begin{aligned} W_5^v(x) = \mathcal{L}\{&s^5\left[(s^2-\gamma_v^2)(s^2-\alpha_v^2)(s^2-\beta_v^2)\right]^{-1}\} = \left[\alpha_v^4(\beta_v^2-\gamma_v^2)ch(\alpha_v x)\right. \\ &\left.+\beta_v^4(\gamma_v^2-\alpha_v^2)ch(\beta_v x) + \gamma_v^4(\alpha_v^2-\beta_v^2)ch(\gamma_v x)\right]/\left[(\alpha_v^2-\beta_v^2)(\alpha_v^2-\gamma_v^2)(\beta_v^2-\gamma_v^2)\right] \end{aligned} \tag{B.14}$$

B.2. Coefficient functions for shear force

$$V_1^v(x) = -m\omega^2(W_1^v(x) + \kappa W_2^v(x))/(c^2\kappa^2) \tag{B.15}$$

$$V_2^v(x) = m\omega^2(W_1^v(x) - \kappa W_2^v(x))/(c^2\kappa^2) \tag{B.16}$$

$$V_3^v(x) = m\omega^2(W_2^v(x) + \kappa W_3^v(x))/(c^2\kappa^2) \tag{B.17}$$

$$V_4^v(x) = m\omega^2(\kappa W_3^v(x) - W_2^v(x))/(c^2\kappa^2) \tag{B.18}$$

$$V_5^{\nu}(x)= m\omega^2(\kappa^2 W_2^{\nu}(x) - W_0^{\nu}(x))/(c^2\kappa^2) \tag{B.19}$$

$$V_6^{\nu}(x)= W_5^{\nu}(x) - W_3^{\nu}(x)/c^2 \tag{B.20}$$

$$V_7^{\nu}(x)= m\omega^2(W_4^{\nu}(x) - W_2^{\nu}(x)/c^2) \tag{B.21}$$

$$V_8^{\nu}(x)= m\omega^2(W_3^{\nu}(x) - W_1^{\nu}(x)/c^2) \tag{B.22}$$

B.3. Coefficient functions for bending deflection

$$w_1^{\nu}(x) = (W_2^{\nu}(x) + \kappa W_3^{\nu}(x))/(c^2\kappa^2) \tag{B.23}$$

$$w_2^{\nu}(x) = (\kappa W_3^{\nu}(x) - W_2^{\nu}(x))/(c^2\kappa^2) \tag{B.24}$$

$$w_3^{\nu}(x)= -(\kappa W_4^{\nu}(x) + W_3^{\nu}(x))/(c^2\kappa^2) \tag{B.25}$$

$$w_4^{\nu}(x) = (W_3^{\nu}(x) - \kappa W_4^{\nu}(x))/(c^2\kappa^2) \tag{B.26}$$

$$w_5^{\nu}(x) = (W_1^{\nu}(x) - \kappa^2 W_3^{\nu}(x))/(c^2 EI) \tag{B.27}$$

$$w_6^{\nu}(x) = (W_0^{\nu}(x) - (L^2+\kappa^2)W_2^{\nu}(x) + L^2\kappa^2 W_4^{\nu}(x))/(c^2 EI\Omega) \tag{B.28}$$

$$w_7^{\nu}(x)= W_5^{\nu}(x) - W_3^{\nu}(x)/c^2 \tag{B.29}$$

$$w_8^{\nu}(x)= W_2^{\nu}(x)/c^2 - W_4^{\nu}(x) \tag{B.30}$$

B.4. Coefficient functions for cross-sectional rotation

$$\begin{aligned}\phi_1^{\nu}(x) = \big[&m\omega^2 L^2(\Phi_1^{\nu}(x) + \kappa\Phi_2^{\nu}(x)) - c^2\Omega EI(\Phi_5^{\nu}(x) + \kappa\Phi_6^{\nu}(x))\\ &+(\Omega EI - m\omega^2\kappa^2 L^2)(\Phi_3^{\nu}(x) + \kappa\Phi_4^{\nu}(x))\big]/(\kappa^2 c^2\Omega EI)\end{aligned} \tag{B.31}$$

$$\begin{aligned}\phi_2^{\nu}(x) = \big[&m\omega^2 L^2(\kappa\Phi_2^{\nu}(x) - \Phi_1^{\nu}(x)) + c^2\Omega EI(\Phi_5^{\nu}(x) - \kappa\Phi_6^{\nu}(x))\\ &+(\Omega EI - m\omega^2\kappa^2 L^2)(\kappa\Phi_4^{\nu}(x) - \Phi_3^{\nu}(x))\big]/(\kappa^2 c^2\Omega EI)\end{aligned} \tag{B.32}$$

$$\phi_3^{\nu}(x)= m\omega^2(\kappa^3\Phi_3^{\nu}(x) + \kappa^2\Phi_2^{\nu}(x) - \kappa\Phi_1^{\nu}(x) - \Phi_0^{\nu}(x))/(\kappa^2 c^2 EI) \tag{B.33}$$

$$\phi_4^{\nu}(x)= m\omega^2(\kappa^3\Phi_3^{\nu}(x) - \kappa^2\Phi_2^{\nu}(x) - \kappa\Phi_1^{\nu}(x) + \Phi_0^{\nu}(x))/(\kappa^2 c^2 EI) \tag{B.34}$$

$$\begin{aligned}\phi_5^{\nu}(x) = \big[&m\omega^2 L^2(\Phi_0^{\nu}(x) - \kappa^2\Phi_2^{\nu}(x)) - c^2\Omega EI(\Phi_4^{\nu}(x) - \kappa^2\Phi_6^{\nu}(x))\\ &+(\Omega EI - m\omega^2\kappa^2 L^2)(\Phi_2^{\nu}(x) - \kappa^2\Phi_4^{\nu}(x))\big]/(\kappa^2 c^2\Omega EI)\end{aligned} \tag{B.35}$$

$$\phi_6^{\nu}(x)= m\omega^2(c^2\kappa^2\Phi_5^{\nu}(x) - (\kappa^2+c^2)\Phi_3^{\nu}(x) + \Phi_1^{\nu}(x))/(c^2 EI) \tag{B.36}$$

$$\phi_7^{\nu}(x)= -m\omega^2(c^2\kappa^2\Phi_4^{\nu}(x) - (\kappa^2+c^2)\Phi_2^{\nu}(x) + \Phi_0^{\nu}(x))/(c^2 EI) \tag{B.37}$$

$$\begin{aligned}\phi_8^{\nu}(x) = \big[&m\omega^2 L^2(\Phi_1^{\nu}(x) - c^2\Phi_3^{\nu}(x)) - c^2\Omega EI(\Phi_5^{\nu}(x) - c^2\Phi_7^{\nu}(x))\\ &+(\Omega EI - m\omega^2\kappa^2 L^2)(\Phi_3^{\nu}(x) - c^2\Phi_5^{\nu}(x))\big]/(c^2\Omega EI)\end{aligned} \tag{B.38}$$

in which,

$$\begin{aligned}\Phi_0^v(x) &= \mathcal{L}\{\left[(c^2s^2-1)(s^2-\gamma_v^2)(s^2-\alpha_v^2)(s^2-\beta_v^2)\right]^{-1}\}\\ &= \frac{sh(\alpha_v x)}{\alpha_v(c^2\alpha_v^2-1)(\alpha_v^2-\beta_v^2)(\alpha_v^2-\gamma_v^2)}+\frac{sh(\beta_v x)}{\beta_v(c^2\beta_v^2-1)(\beta_v^2-\gamma_v^2)(\beta_v^2-\alpha_v^2)}\\ &+\frac{sh(\gamma_v x)}{\gamma_v(c^2\gamma_v^2-1)(\gamma_v^2-\alpha_v^2)(\gamma_v^2-\beta_v^2)}-\frac{c^5sh(x/c)}{(c^2\alpha_v^2-1)(c^2\beta_v^2-1)(c^2\gamma_v^2-1)}\end{aligned} \tag{B.39}$$

$$\begin{aligned}\Phi_1^v(x) &= \mathcal{L}\{s\left[(c^2s^2-1)(s^2-\gamma_v^2)(s^2-\alpha_v^2)(s^2-\beta_v^2)\right]^{-1}\}\\ &= \frac{ch(\alpha_v x)}{(c^2\alpha_v^2-1)(\alpha_v^2-\beta_v^2)(\alpha_v^2-\gamma_v^2)}+\frac{ch(\beta_v x)}{(c^2\beta_v^2-1)(\beta_v^2-\gamma_v^2)(\beta_v^2-\alpha_v^2)}\\ &+\frac{ch(\gamma_v x)}{(c^2\gamma_v^2-1)(\gamma_v^2-\alpha_v^2)(\gamma_v^2-\beta_v^2)}-\frac{c^4ch(x/c)}{(c^2\alpha_v^2-1)(c^2\beta_v^2-1)(c^2\gamma_v^2-1)}\end{aligned} \tag{B.40}$$

$$\begin{aligned}\Phi_2^v(x) &= \mathcal{L}\{s^2\left[(c^2s^2-1)(s^2-\gamma_v^2)(s^2-\alpha_v^2)(s^2-\beta_v^2)\right]^{-1}\}\\ &= \frac{\alpha_v sh(\alpha_v x)}{(c^2\alpha_v^2-1)(\alpha_v^2-\beta_v^2)(\alpha_v^2-\gamma_v^2)}+\frac{\beta_v sh(\beta_v x)}{(c^2\beta_v^2-1)(\beta_v^2-\gamma_v^2)(\beta_v^2-\alpha_v^2)}\\ &+\frac{\gamma_v sh(\gamma_v x)}{(c^2\gamma_v^2-1)(\gamma_v^2-\alpha_v^2)(\gamma_v^2-\beta_v^2)}-\frac{c^3sh(x/c)}{(c^2\alpha_v^2-1)(c^2\beta_v^2-1)(c^2\gamma_v^2-1)}\end{aligned} \tag{B.41}$$

$$\begin{aligned}\Phi_3^v(x) &= \mathcal{L}\{s^3\left[(c^2s^2-1)(s^2-\gamma_v^2)(s^2-\alpha_v^2)(s^2-\beta_v^2)\right]^{-1}\}\\ &= \frac{\alpha_v^2 ch(\alpha_v x)}{(c^2\alpha_v^2-1)(\alpha_v^2-\beta_v^2)(\alpha_v^2-\gamma_v^2)}+\frac{\beta_v^2 ch(\beta_v x)}{(c^2\beta_v^2-1)(\beta_v^2-\gamma_v^2)(\beta_v^2-\alpha_v^2)}\\ &+\frac{\gamma_v^2 ch(\gamma_v x)}{(c^2\gamma_v^2-1)(\gamma_v^2-\alpha_v^2)(\gamma_v^2-\beta_v^2)}-\frac{c^2ch(x/c)}{(c^2\alpha_v^2-1)(c^2\beta_v^2-1)(c^2\gamma_v^2-1)}\end{aligned} \tag{B.42}$$

$$\begin{aligned}\Phi_4^v(x) &= \mathcal{L}\{s^4\left[(c^2s^2-1)(s^2-\gamma_v^2)(s^2-\alpha_v^2)(s^2-\beta_v^2)\right]^{-1}\}\\ &= \frac{\alpha_v^3 sh(\alpha_v x)}{(c^2\alpha_v^2-1)(\alpha_v^2-\beta_v^2)(\alpha_v^2-\gamma_v^2)}+\frac{\beta_v^3 sh(\beta_v x)}{(c^2\beta_v^2-1)(\beta_v^2-\gamma_v^2)(\beta_v^2-\alpha_v^2)}\\ &+\frac{\gamma_v^3 sh(\gamma_v x)}{(c^2\gamma_v^2-1)(\gamma_v^2-\alpha_v^2)(\gamma_v^2-\beta_v^2)}-\frac{csh(x/c)}{(c^2\alpha_v^2-1)(c^2\beta_v^2-1)(c^2\gamma_v^2-1)}\end{aligned} \tag{B.43}$$

$$\begin{aligned}\Phi_5^v(x) &= \mathcal{L}\{s^5\left[(c^2s^2-1)(s^2-\gamma_v^2)(s^2-\alpha_v^2)(s^2-\beta_v^2)\right]^{-1}\}\\ &= \frac{\alpha_v^4 ch(\alpha_v x)}{(c^2\alpha_v^2-1)(\alpha_v^2-\beta_v^2)(\alpha_v^2-\gamma_v^2)}+\frac{\beta_v^4 ch(\beta_v x)}{(c^2\beta_v^2-1)(\beta_v^2-\gamma_v^2)(\beta_v^2-\alpha_v^2)}\\ &+\frac{\gamma_v^4 ch(\gamma_v x)}{(c^2\gamma_v^2-1)(\gamma_v^2-\alpha_v^2)(\gamma_v^2-\beta_v^2)}-\frac{ch(x/c)}{(c^2\alpha_v^2-1)(c^2\beta_v^2-1)(c^2\gamma_v^2-1)}\end{aligned} \tag{B.44}$$

$$\begin{aligned}\Phi_6^v(x) &= \mathcal{L}\{s^6\left[(c^2s^2-1)(s^2-\gamma_v^2)(s^2-\alpha_v^2)(s^2-\beta_v^2)\right]^{-1}\}\\ &= \frac{\alpha_v^5 sh(\alpha_v x)}{(c^2\alpha_v^2-1)(\alpha_v^2-\beta_v^2)(\alpha_v^2-\gamma_v^2)}+\frac{\beta_v^5 sh(\beta_v x)}{(c^2\beta_v^2-1)(\beta_v^2-\gamma_v^2)(\beta_v^2-\alpha_v^2)}\\ &+\frac{\gamma_v^5 sh(\gamma_v x)}{(c^2\gamma_v^2-1)(\gamma_v^2-\alpha_v^2)(\gamma_v^2-\beta_v^2)}-\frac{sh(x/c)}{c(c^2\alpha_v^2-1)(c^2\beta_v^2-1)(c^2\gamma_v^2-1)}\end{aligned} \tag{B.45}$$

$$\begin{aligned}\Phi_7^v(x) &= \mathcal{L}\{s^7\left[(c^2s^2-1)(s^2-\gamma_v^2)(s^2-\alpha_v^2)(s^2-\beta_v^2)\right]^{-1}\}\\ &= \frac{\alpha_v^6 ch(\alpha_v x)}{(c^2\alpha_v^2-1)(\alpha_v^2-\beta_v^2)(\alpha_v^2-\gamma_v^2)}+\frac{\beta_v^6 ch(\beta_v x)}{(c^2\beta_v^2-1)(\beta_v^2-\gamma_v^2)(\beta_v^2-\alpha_v^2)}\\ &+\frac{\gamma_v^6 ch(\gamma_v x)}{(c^2\gamma_v^2-1)(\gamma_v^2-\alpha_v^2)(\gamma_v^2-\beta_v^2)}-\frac{ch(x/c)}{c^2(c^2\alpha_v^2-1)(c^2\beta_v^2-1)(c^2\gamma_v^2-1)}\end{aligned} \tag{B.46}$$

References

[1] L. Que, J.S. Park, Y.B. Gianchandani, Bent-beam electrothermal actuators – Part I: single beam and cascaded devices, J. Microelectromech. Syst. 10 (2001) 247–254.
[2] Z.-B. Shen, X.-F. Li, L.-P. Sheng, G.-J. Tang, Transverse vibration of nanotube-based micro-mass sensor via nonlocal Timoshenko beam theory, Comput. Mater. Sci. 53 (2012) 340–346.
[3] N. Kacem, S. Hentz, D. Pinto, B. Reig, V. Nguyen, Nonlinear dynamics of nanomechanical beam resonators: improving the performance of NEMS-based sensors, Nanotechnology 20 (2009).
[4] Y.A. Pashkin, Y. Nakamura, J.S. Tsai, Room-temperature Al single-electron transistor made by electron-beam lithography, Appl. Phys. Lett. 76 (2000) 2256–2258.
[5] J.E. Sader, J.W.M. Chon, P. Mulvaney, Calibration of rectangular atomic force microscope cantilevers, Rev. Sci. Instrum. 70 (1999) 3967–3969.
[6] G. Stan, C.V. Ciobanu, P.M. Parthangal, R.F. Cook, Diameter-dependent radial and tangential elastic moduli of ZnO nanowires, Nano Lett. 7 (2007) 3691–3697.
[7] C. Motz, D. Weygand, J. Senger, P. Gumbsch, Micro-bending tests: A comparison between three-dimensional discrete dislocation dynamics simulations and experiments, Acta Mater. 56 (2008) 1942–1955.
[8] K. Asano, H.C. Tang, C.Y. Chen, T. Nagoshi, T.F.M. Chang, D. Yamane, K. Machida, K. Masu, M. Sone, Micro-bending testing of electrodeposited gold for applications as movable components in MEMS devices, Microelectron. Eng. 180 (2017) 15–19.
[9] J. Cai, Y.-L. Li, D. Mo, Y.-D. Wang, Softening effect on elastic moduli of Fe, Nb, Cu, and RuAl nanoparticles, J. Nanosci. Nanotechnol. 19 (2019) 7899–7905.
[10] W.T. Koiter, Couple stresses in the theory of elasticity, I and II, Proc. Ser. B, K. Ned. Akad. Wet. 67 (1964) 17–44.
[11] R.A. Toupin, Elastic materials with couple stresses, Arch. Ration. Mech. Anal. 11 (1962) 385–414.
[12] R.D. Mindlin, H.F. Tiersten, Effects of couple-stresses in linear elasticity, Arch. Ration. Mech. Anal. 11 (1962) 415–448.
[13] R.D. Mindlin, Second gradient of strain and surface-tension in linear elasticity, Int. J. Solids Struct. 1 (1965) 417–438.
[14] R.D. Mindlin, N.N. Eshel, On first strain-gradient theories in linear elasticity, Int. J. Solids Struct. 4 (1968) 109–124.
[15] D.C.C. Lam, F. Yang, A.C.M. Chong, J. Wang, P. Tong, Experiments and theory in strain gradient elasticity, J. Mech. Phys. Solids 51 (2003) 1477–1508.
[16] F. Yang, A.C.M. Chong, D.C.C. Lam, P. Tong, Couple stress based strain gradient theory for elasticity, Int. J. Solids Struct. 39 (2002) 2731–2743.
[17] S.E. Alavi, M. Sadighi, M.D. Pazhooh, J.-F. Ganghoffer, Development of size-dependent consistent couple stress theory of Timoshenko beams, Appl. Math. Model. 79 (2020) 685–712.
[18] A. Andakhshideh, R. Rafiee, S. Maleki, 3D stress analysis of generally laminated piezoelectric plates with electromechanical coupling effects, Appl. Math. Model. 74 (2019) 258–279.
[19] M.R. Ghazavi, H. Molki, A.A. Beigloo, Nonlinear analysis of the micro/nanotube conveying fluid based on second strain gradient theory, Appl. Math. Model. 60 (2018) 77–93.
[20] X. Ji, A. Li, S. Zhou, A comparison of strain gradient theories with applications to the functionally graded circular micro-plate, Appl. Math. Model. 49 (2017) 124–143.
[21] A. Li, X. Ji, S. Zhou, L. Wang, J. Chen, P. Liu, Nonlinear axisymmetric bending analysis of strain gradient thin circular plate, Appl. Math. Model. 89 (2021) 363–380.
[22] M.H. Shojaeefard, H.S. Googarchin, M. Ghadiri, M. Mahinzare, Micro temperature-dependent FG porous plate: free vibration and thermal buckling analysis using modified couple stress theory with CPT and FSDT, Appl. Math. Model. 50 (2017) 633–655.
[23] E. Kröner, Elasticity theory of materials with long range cohesive forces, Int. J. Solids Struct. 3 (1967) 12.
[24] A.C. Eringen, D.G.B. Edelen, On nonlocal elasticity, Int. J. Eng. Sci. 10 (1972) 233–248.
[25] A.C. Eringen, On differential equations of nonlocal elasticity and solutions of screw dislocation and surface waves, J. Appl. Phys. 54 (1983) 4703–4710.
[26] P.-L. Bian, H. Qing, C.-F. Gao, One-dimensional stress-driven nonlocal integral model with bi-Helmholtz kernel: close form solution and consistent size effect, Appl. Math. Model. 89 (2021) 400–412.
[27] S. Faroughi, A. Rahmani, M.I. Friswell, On wave propagation in two-dimensional functionally graded porous rotating nano-beams using a general nonlocal higher-order beam model, Appl. Math. Model 80 (2020) 169–190.
[28] M. Ganapathi, O. Polit, A nonlocal higher-order model including thickness stretching effect for bending and buckling of curved nanobeams, Appl. Math. Model. 57 (2018) 121–141.
[29] E. Mahmoudpour, S.H. Hosseini-Hashemi, S.A. Faghidian, Nonlinear vibration analysis of FG nano-beams resting on elastic foundation in thermal environment using stress-driven nonlocal integral model, Appl. Math. Model. 57 (2018) 302–315.
[30] P. Moradweysi, R. Ansari, K. Hosseini, F. Sadeghi, Application of modified Adomian decomposition method to pull-in instability of nano-switches using nonlocal Timoshenko beam theory, Appl. Math. Model. 54 (2018) 594–604.
[31] Y. Yuan, K. Xu, K. Kiani, Torsional vibration of nonprismatically nonhomogeneous nanowires with multiple defects: surface energy-nonlocal-integro-based formulations, Appl. Math. Model. 82 (2020) 17–44.
[32] C.W. Lim, G. Zhang, J.N. Reddy, A higher-order nonlocal elasticity and strain gradient theory and its applications in wave propagation, J. Mech. Phys. Solids 78 (2015) 298–313.
[33] F. Ebrahimi, M.R. Barati, Hygrothermal effects on vibration characteristics of viscoelastic FG nanobeams based on nonlocal strain gradient theory, Compos. Struct. 159 (2017) 433–444.
[34] F. Ebrahimi, M.R. Barati, A nonlocal strain gradient refined beam model for buckling analysis of size-dependent shear-deformable curved FG nanobeams, Compos. Struct. 159 (2017) 174–182.
[35] S. Sahmani, M.M. Aghdam, Nonlocal strain gradient beam model for nonlinear vibration of prebuckled and postbuckled multilayer functionally graded GPLRC nanobeams, Compos. Struct. 179 (2017) 77–88.
[36] S. Sahmani, M.M. Aghdam, T. Rabczuk, Nonlinear bending of functionally graded porous micro/nano-beams reinforced with graphene platelets based upon nonlocal strain gradient theory, Compos. Struct. 186 (2018) 68–78.
[37] G.-L. She, F.-G. Yuan, Y.-R. Ren, H.-B. Liu, W.-S. Xiao, Nonlinear bending and vibration analysis of functionally graded porous tubes via a nonlocal strain gradient theory, Compos. Struct. 203 (2018) 614–623.
[38] Y. Gao, W.S. Xiao, H.P. Zhu, Nonlinear vibration of functionally graded nano-tubes using nonlocal strain gradient theory and a two-steps perturbation method, in: Struct. Eng. Mech., 69, 2019, pp. 205–219.
[39] M. Al-shujairi, C. Mollamahmutoglu, Dynamic stability of sandwich functionally graded micro-beam based on the nonlocal strain gradient theory with thermal effect, Compos. Struct. 201 (2018) 1018–1030.
[40] H. Liu, Z. Lv, H. Wu, Nonlinear free vibration of geometrically imperfect functionally graded sandwich nanobeams based on nonlocal strain gradient theory, Compos. Struct. 214 (2019) 47–61.
[41] S. Guo, Y. He, D. Liu, J. Lei, Z. Li, Dynamic transverse vibration characteristics and vibro-buckling analyses of axially moving and rotating nanobeams based on nonlocal strain gradient theory, Microsyst. Technol.-Micro- Nanosyst.-Inf. Storage Process. Syst. 24 (2018) 963–977.
[42] L. Lu, X. Guo, J. Zhao, A unified size-dependent plate model based on nonlocal strain gradient theory including surface effects, Appl. Math. Model. 68 (2019) 583–602.
[43] L. Li, Y. Hu, Nonlinear bending and free vibration analyses of nonlocal strain gradient beams made of functionally graded material, Int. J. Eng. Sci. 107 (2016) 77–97.
[44] L. Li, X. Li, Y. Hu, Free vibration analysis of nonlocal strain gradient beams made of functionally graded material, Int. J. Eng. Sci. 102 (2016) 77–92.
[45] M. Mohammadian, M.H. Abolbashari, S.M. Hosseini, Application of hetero junction CNTs as mass nanosensor using nonlocal strain gradient theory: an analytical solution, Appl. Math. Model. 76 (2019) 26–49.

[46] B. Karami, M. Janghorban, T. Rabczuk, Dynamics of two-dimensional functionally graded tapered Timoshenko nanobeam in thermal environment using nonlocal strain gradient theory, Compos. Part B-Eng. 182 (2020).
[47] M. Mir, M. Tahani, Graphene-based mass sensors: chaotic dynamics analysis using the nonlocal strain gradient model, Appl. Math. Model. 81 (2020) 799–817.
[48] R. Zaera, O. Serrano, J. Fernandez-Saez, On the consistency of the nonlocal strain gradient elasticity, Int. J. Eng. Sci. 138 (2019) 65–81.
[49] C. Li, H. Qing, C. Gao, Theoretical analysis for static bending of Euler-Bernoulli beam using different nonlocal gradient models, Mech. Adv. Mater. Struct. 20 (2020) 912–934.
[50] Y. Benveniste, A new approach to the application of Mori-Tanaka's theory in composite materials, Mech. Mater. 6 (1987) 147–157.
[51] P.-L. Bian, H. Qing, On bending consistency of Timoshenko beam using differential and integral nonlocal strain gradient models, ZAMM-Z. Angew. Math. Mech. (2021).
[52] L.-l. Jing, P.-j. Ming, W.-p. Zhang, L.-r. Fu, Y.-p. Cao, Static and free. vibration analysis of functionally graded beams by combination Timoshenko theory and finite volume method, Compos. Struct. 138 (2016) 192–213.
[53] A. Apuzzo, R. Barretta, S.A. Faghidian, R. Luciano, F.M. de Sciarra, Free vibrations of elastic beams by modified nonlocal strain gradient theory, Int. J. Eng. Sci. 133 (2018) 99–108.